BERICHTE
aus dem MARUM und dem Fachbereich Geowissenschaften der Universität Bremen

No. 300

Bohrmann, G., A. Aljuhne, K. Dehning, C. Ferreira, T. Feseker, E.S. Gürcan, E. Hacioğlu, T. Leymann, G. Meinecke, T. Pape, J. Renken, M. Roemer, U. Spiesecke, T. v.Wahl

Report and Preliminary Results of R/V POSEIDON Cruise P462, Izmir - Izmir, 28 October - 21 November, 2013

Gas Hydrate Dynamics of Mud Volcanoes in the Submarine Anaximander Mountains (Eastern Mediterranean)

Berichte, MARUM – Zentrum für Marine Umweltwissenschaften, Fachbereich Geowissenschaften, Universität Bremen, No. 300, 51 pages, Bremen 2014

ISSN 2195-9633

Berichte aus dem MARUM und dem Fachbereich Geowissenschaften der Universität Bremen

published by

MARUM – Center for Marine Environmental Sciences
Leobener Strasse, 28359 Bremen, Germany
www.marum.de

and

Fachbereich Geowissenschaften der Universität Bremen
Klagenfurter Strasse, 28359 Bremen, Germany
www.geo.uni-bremen.de

The "Berichte aus dem MARUM und dem Fachbereich Geowissenschaften der Universität Bremen" appear at irregular intervals and serve for the publication of cruise, project and technical reports arising from the scientific work by members of the publishing institutions.

Citation:

Bohrmann, G., A. Aljuhne, K. Dehning, C. Ferreira, T. Feseker, E.S. Gürcan, E. Hacioğlu, T. Leymann, G. Meinecke, T. Pape, J. Renken, M. Roemer, U. Spiesecke, T. v.Wahl. Report and Preliminary Results of R/V POSEIDON Cruise P462, Izmir – Izmir, 28 October – 21 November, 2013. Gas Hydrate Dynamics of Mud Volcanoes in the Submarine Anaximander Mountains (Eastern Mediterranean). Berichte, MARUM – Zentrum für Marine Umweltwissenschaften, Fachbereich Geowissenschaften, Universität Bremen, No. 300, 51 pages. Bremen, 2013. ISSN 2195-9633.

An electronic version of this report can be downloaded from:
http://nbn-resolving.de/urn:nbn:de:gbv:46-MARUM9

Printed copies can be ordered from: Monika Bachur, MARUM – Center for Marine Environmental Sciences, University of Bremen, Leobener Strasse, 28359 Bremen, Germany
Phone: (49) 421 218-65516 │ Fax: (49) 421 218-9865516 │ e-mail: MBachur@marum.de

For editorial concerns please contact reports@marum.de

R/V POSEIDON
Cruise Report P462

Gas Hydrate Dynamics of Mud Volcanoes in the Submarine Anaximander Mountains (Eastern Mediterranean)

P462
Izmir – Izmir
28 October – 21 November, 2013

Cruise sponsored by Deutsche Forschungsgemeinschaft (DFG)

Edited by
Gerhard Bohrmann and Greta Ohling
With contributions of cruise participants

The cruise was performed by
MARUM – Center for Marine Environmental Sciences

marum

Universität Bremen

R/V POSEIDON Cruise Report P462

Table of Contents

1 Preface

R/V POSEIDON cruise P462 to the Anaximander Mountains was planned, coordinated and carried out by MARUM Center for Marine Environmental Sciences at the University of Bremen. The research program is part of the DFG Research Center and Cluster of Excellence "The Ocean in the Earth System" in Research Area "Geosphere Biosphere Interactions", project GB3 "Contribution of Cold Seeps to Geological Processes, Carbon Fluxes, and Ecosystem Diversity". The cruise was financed by the German Research Foundation (DFG) within GB3 and by an incentive fund proposal "Anaximander Mud volcanoes". The shipping operator Reederei Briese Schiffahrts GmbH & Co KG provided technical support on the vessel. We would like to specially acknowledge the master of the vessel, Matthias Günther and his crew for their continued contribution to a pleasant and professional atmosphere aboard R/V POSEIDON.

Fig. 1: Scientific crew aboard R/V POSEIDON P462

Personel aboard R/V POSEIDON

Table 1: Scientific crew

Name	Discipline	Affiliation	Leg
Ammar Aljuhne	Multibeam	MARUM	2
Gerhard Bohrmann	Chief scientist	GeoBremen	1
Klaus Dehning	DAPC, coring	MARUM	1
Christian Ferreira	Multibeam	MARUM	1 & 2
Tom Feseker	Observatories	GeoBremen	2
Elif Seda Gürcan	Observer[1)]	University Sinop	1
Ekrem Hacioğlu	Observer	MTA, Ankara	1 & 2
Tom Leymann	AUV SEAL	MARUM	2
Gerrit Meinecke	AUV, chief scientist	MARUM	1 & 2
Thomas Pape	Sediments, gas samples	GeoBremen	1
Jens Renken	AUV SEAL	MARUM	1 & 2
Miriam Römer	Mapping, GIS, sediments	GeoBremen	1 & 2
Ulli Spiesecke	AUV SEAL	MARUM	1 & 2
Till von Wahl	AUV SEAL	MARUM	1 & 2

[1)] Elif Seda Gürcan was disembarked in Antalya on Sunday 3 November

MARUM	Center for Marine and Environmental Sciences, DFG Research Center and Cluster of Excellence, University of Bremen, Postfach 330440, 28334 Bremen, **Germany**
GeoB	Department of Geosciences, University of Bremen, Klagenfurter Str., 28359 Bremen, **Germany**
MTA	Department of Marine and Environmental Research, General directorate of mineral research and exploration, Üniversiteler Mahallesi Dumlupinar Bulv. No: 139, 06800 Cankaya/Ankara, **Turkey**
Sinop, Uni	University of Sinop, Sinop Üniversitesi Su Ürünleri Fakültesi, Rektörlügü, 57000 Sinop, **Turkey**

Table 2: Crew members onboard

Name	**Discipline**
Matthias Günther	Master
Dirk Thürsam	Chief officer
Hero Nannen	2nd officer
Kurre-Klas Kröger	Chief engineer
Hans-Jörg Freund	2nd engineer
Dietmar Klare	Electrician
Rüdiger Engel	Seaman
Frank Schrage	Bosun
Ronald Kuhn	Seaman
Bernd Rauh	Seaman
Roland Heyne	Seaman
Benjamin Brüdigam	Seaman
Felix Meyer	Seaman
Wilfried Kluge	Cook
Bernd Gerischewski	Steward

Shipping operator: Briese Schiffahrts GmbH & Co KG, Abteilung Forschungsschifffahrt, Hafenstr. 12, 26789 Leer, **Germany**

2 Introduction

2.1 Objectives, Background and Research Program

(G. Bohrmann)

The prime objective of the research in the investigation area of the "Anaximander Mountains" south of Turkey (Fig. 2) was to decipher key processes of mud volcanoes. In contrast to many other mud volcanoes in the Mediterranean Sea, mud volcanoes of the Anaximander Mountains reveal gas hydrates in shallow marine sediments (Lykousis et al. 2009, Pape et al. 2010, Perissoratis et al. 2011).

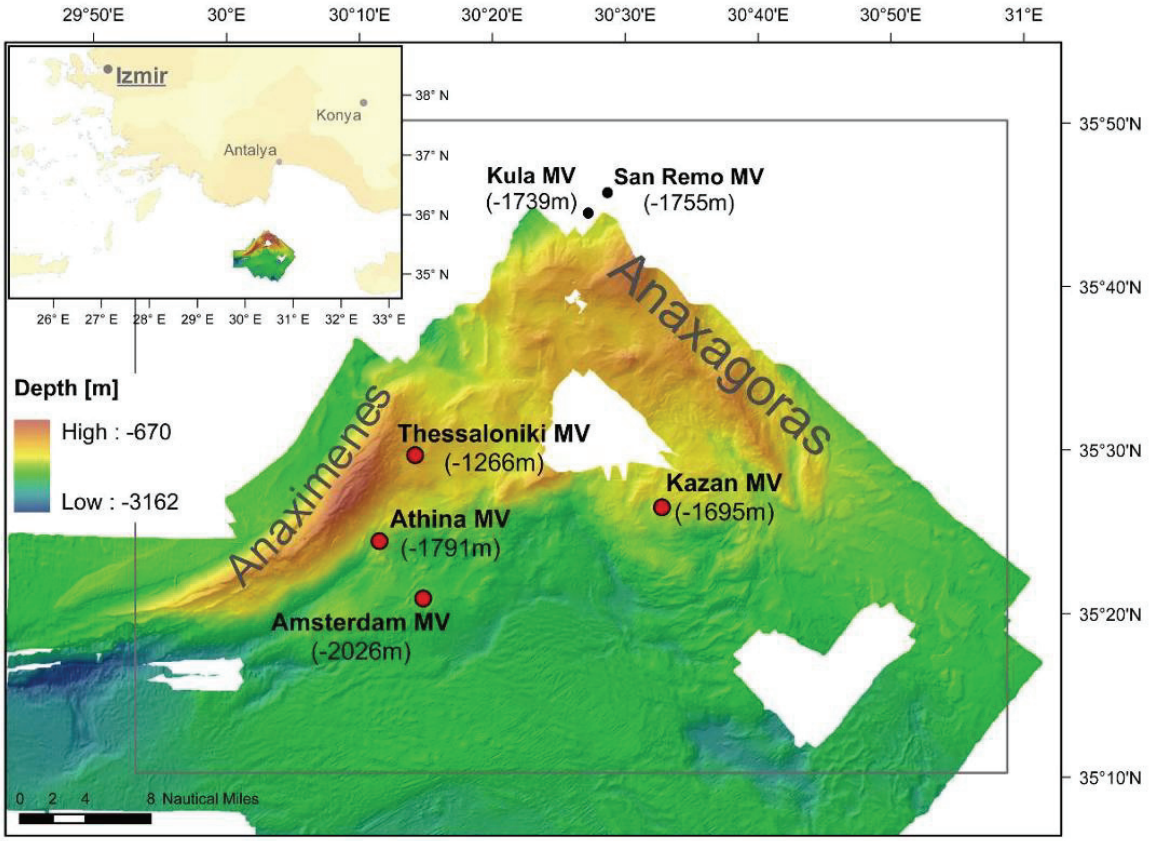

Fig. 2: Bathymetric map of R/V METEOR cruise M70/3, and positions of major mud volcanoes in the Anaximander Mountains. The working area comprises the Anaximenes and the Anaxagoras Highs. Target MVs are highlighted by red dots. Insert: Location of the working area in the Anaximander Mountains south of Turkey.

Investigations in the Anaximander area prior to this cruise have documented methane seeps at several mud volcanoes in about 2000 m water depth. Gas hydrates exist in the sediments of the mud volcanoes and there was strong evidence that at some of the structures methane escapes as gas from the sea floor. The main objective of the R/V POSEIDON cruise P462 was to perform a couple of AUV dives during which the micro-bathymetry of four mud volcanoes will be measured in order to get a more or less full coverage of these structures. After post-processing the multibeam 3D models from high resolution data should image the detailed micro-morphology of the mud volcanoes. This information is highly requested for detailed sampling of the mud volcanoes as well as to get deep insight into the construction of the mud extrusion build-ups. The micro-bathymetry data are specifically requested for future ROV dives on these mud volcanoes, which are planned with MARUM

ROV-QUEST 4000 in 2-3 years. The proposal for the ROV work (MerMet 13-43) is already confirmed by the DFG commission for oceanography with 26 working days.

The proposed research is aimed to investigating the distribution of natural gas hydrates in relation to pressure, temperature, gas chemistry, and pore fluid salinity at deep-sea mud volcanoes in the Eastern Mediterranean Sea. Currently, only few details are known about the characteristics of hydrate systems in the Mediterranean. Located at depths between 1,260 and 2,030 m below sea level, the four target MVs in the Anaximander mountains (Thessaloniki Mud Volcano = TMV, Kazan Mud Volcano = KMV, Athena Mud Volcano = AthMV, and Amsterdam Mud Volcano = AMV) cover a large pressure interval of about 77 bar within the GHSZ for both, structure I and II hydrates (Fig. 3).

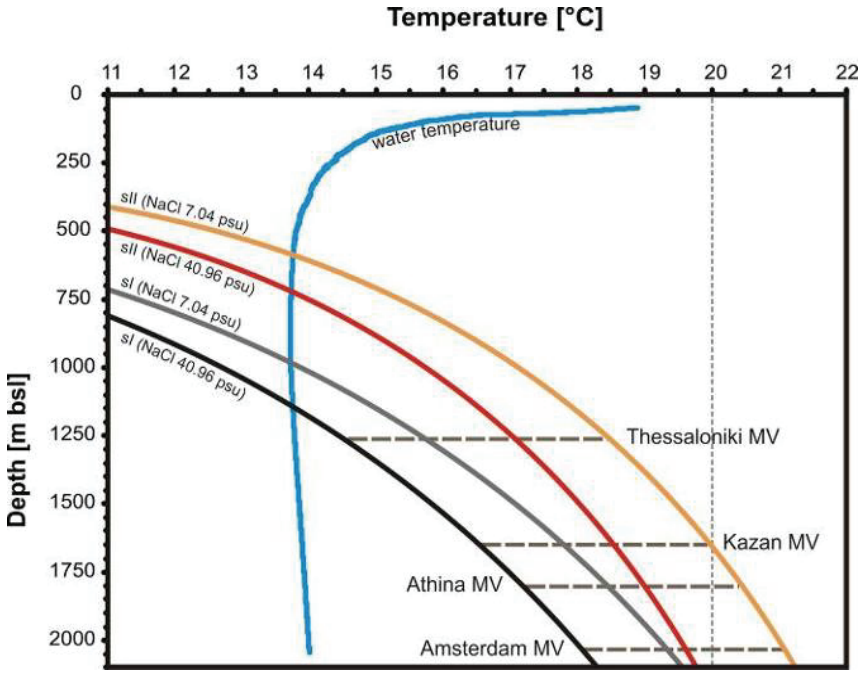

Fig. 3: Phase boundaries of sI and sII hydrates for the assuming hydrocarbon compositions and low-saline pore fluid (7.04 psu) identical to fluids at the Amsterdam MV (Pape et al. 2010). Phase boundaries of sI and sII at salinities of Mediterranean bottom waters (40.96 psu) are shown for reference. The horizontal dashed lines depict the water depth of the selected mud volcanoes.

Although hydrates might be generally stable in their physico-chemical setting the top of hydrates will always be subject to dissolution due to the methane concentration gradient. Therefore, hydrates might form a constant source of methane to the overlying sediment column. Considering temperature and pressure conditions at the Amsterdam Mud Volcano in 2006 (M70/3), our calculations demonstrate that hydrates are well within the limits of the GHSZ. Because of the dissolution of the uppermost hydrate layers, they are likely to provide a constant methane source into overlying sediments and to communities mediating the anaerobic oxidation of methane (AOM). By-products of the AOM migrating towards the seafloor are consumed by chemosynthetic symbionts hosted by benthic organisms such as polychaetes and bivalves. The correlation of chemosynthetic biomass on the seafloor and methane hydrates below in the sediments will be investigated.

A further goal is to correlate hydrate presence in the pore space (pressure cores) with temperature data (heat flow probe), and composition of sediments and pore fluids. Molecular compositions of gas present in shallow MV deposits might vary depending on the distance to the

conduit due to the extent of fractionation during hydrate formation and the microbial consumption of light hydrocarbons especially in the sulfate-methane-interface. Co-existences of sI and sII hydrates have already been proposed for the Amsterdam mud volcano as a result of the works performed during M70/3 (Pape et al. 2010). Hence, the gas composition will be correlated with hydrate structures (from GC-T) at specific sites in order to characterize their sensitivity to temperature increases resulting from mud volcanic eruption.

Fig. 4: Research tools used during cruise P462. R/V POSEIDON in the port of Izmir, Turkey (above left); AUV SEAL 5000 m on the working deck during the launching (above right); conventional gravity corer comes back from the seafloor (below left) and the autoclave piston corer (DAPC) deployed from the vessel.

Due to mud volcanic activity, sediment temperatures at the Amsterdam mud volcano range between the bottom water temperature of about 13.8°C and up to more than 20°C within the upper sediment that can be reached by gravity corers and DAPC. Dissociation temperatures for sI hydrate are ca. 19.3°C (at 7.04 psu), while sII would decompose at ca. 21.1°C. Consequently, the hydrates at the target MVs are close to their stability limits and likely to be subject to partial dissociation during pulses of increased activity. In situ sediment temperatures will be correlated with the presence/ absence of hydrates and their crystallographic structure. The knowledge of the specific role of an individual parameter (gas composition, pore water salinity, sediment temperature) and their interplay for the spatial hydrate distribution will be used to model the hydrate dynamics during the different phases of mud volcanic activity and to estimate the methane amounts stored and released at the target mud volcanoes.

The following scientific questions were addressed during the cruise:

- How different are the mud volcanoes in their construction?
- Are there relative fresh mud flows which can be identified and how are the shallow gas hydrates associated to those recent flows?
- Are the hydrates in older or younger sediments?
- Are there differences in hydrate concentrations for different lithologies e.g. pure mud, or mud breccias?
- Which conditions control the escape of fluids (liquid, gas) and mud and how does this shape the appearance of the seeps?
- How much methane is escaping as gas bubbles from the sea floor to the water column?
- What is the advective fluid flow and what is the source of the fluids?
- How much gas and gas hydrates exist in the sediments?
- Which organisms live at the seeps?

2.2 Geological Setting of the Anaximander Mountains

The Anaximander Mountains are located on the northeastern flank of the Mediterranean Ridge at water depths of ca. 1,200 to 2,050 m. There are three morphologically elevated areas (Anaximander sensu strictu and Anaximenes in the western part, Anaxagoras in the eastern part). A general compressional tectonic regime due to the convergence between the African and Eurasian plates has led to fluid circulation and mud extrusion (Limonov et al., 1996; Woodside et al., 1998). Currently, the Anaximander Mountains are undergoing neotectonic deformation (Huguen et al., 2005; Zitter et al., 2003). The Anaximander Mountains are known to host numerous active mud volcanic structures at water depths between about 1,260 and 2,030 mbsl. Several mud volcanoes, like the Kula MV, the Kazan MV, the Amsterdam MV, the Athina MV (Fig. 2) have already been investigated with regard to tectonic setting, pore fluid chemistry, micro- and macro-organisms, and hydrate occurrences (Aloisi et al., 2000; Charlou et al., 2003; Lykousis et al., 2009; Woodside et al., 1998). The first discovery of intact hydrates at the Kula MV in the Anaximander Mountains during a cruise in 1996 (Woodside et al., 1998) was followed by findings at other MVs in the same region more recently (e.g. Lykousis et al., 2004, 2009; Pape et al., 2010b; Zitter et al., 2005).

The Anaximander mountains represent the offshore continuation of the geological units exposed onshore southwest of Turkey. According to lithological and geological correlation, Anaximander and Anaximanes mountains are located on the Beydag Unit. The Anaxagoras mountains are located in continuation of the Antalya nappe. The Beydag Unit was named by an area in Turkey west of Tauros. This unit is composed of upper Triassic to upper Cretaceous rocks. Triassic sediments are represented mostly by clastic and fine grained deposits. Upper Jurassic and lower Cretaceous sediments represent lagoonal environments and have excellent source rock potential. The Antalya nappe complex comprises ophiolitic melange, ophiolitic sequences, and medium to high grade metamorphic rocks of the Mesozoic clastic deposits and carbonates.

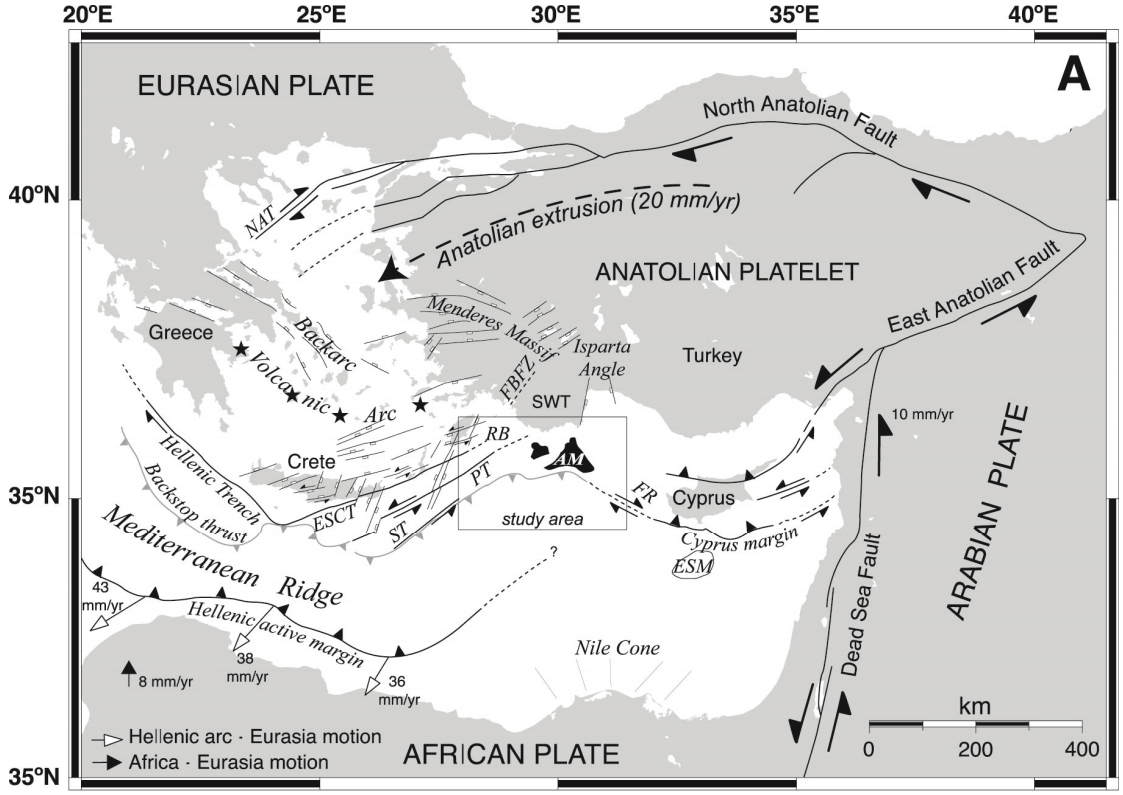

Fig. 5: Geodynamic framework of the eastern Mediterranean from Zitter et al., 2005. The motion vector of Africa is from DeMets et al. (1994) and the southwestward motion of the Hellenic Arc relative to Eurasia is from McClusky et al. (2000). The Hellenic forearc from Crete to Rhodes shows a strain pattern with N70°E-striking strike-slip faults and N20°E-striking normal faults, resulting from transtensional deformation since the Pliocene. The dextral shearing shown along the Florence Rise was inferred by Woodside et al. (2002). New results require the sense of shear in this locality to be sinistral instead. Abbreviations: ESCT = East South Cretan Trough, ST = Strabo Trench; PT = Pliny Trench; RB = Rhodes Basin; AM = Anaximander Mountains; FR = Florence Rise; ESM = Erasthothenes Seamount; FBFZ = the hypothetical Fethiye-Burdur Fault Zone; SWT = Southwest Turkey; NAT = North Aegean Trough. Stars indicate subduction-related Quaternary volcanism.

The Antalya Neogen basin is surrounded by the Antalya nappe complex. This area which is located in the southern part of Turkey, is characterized by northeast dipped sedimentary units. The area is NW/SE oriented and has an elongated shape. The thickness of the Neogene sedimentary units comprise more than 2000 m sediments. The thickness and dipping of the sedimentary units increases to the north and continues in the northern sector (Huguen et al., 2005). After the Early-Middle Miocene eastern sector emplacement of the Lycian nappes, Servalian and Tortonian was characterized by the development of graben structures (Dewey and Sengor, 1970). In the eastern Mediterranean offshore of Turkey, turbiditic facies are dominated in late Langian to Serravalian stage and Tortonian deposits are represented by thick fluvial and deltaic facies. The Anaximander Mountains which are situated in the southern sector of Finike Basin (Fig. 6) are located at the junction of Hellenic and Cyprus arcs (Fig. 6). This sector is located south-east of the Finike basin, and is a western part of the Antalya basin (Fig. 6). A different tectonic style started in late Miocene and the seamounts in the Anaximander area started to become formed in this stage. The Messinian and early Quaternary units around the Anaximander mountains are characterized by dextral strike-slip faults by onset of an extension on NE oriented normal faults and a depression (Huguen et al., 2005).

Ophiolitic rocks were observed in the southeast of the Finike basin, and have extension to the north. It is known that in the northeast part of the Anaxagoras mountains a melange is present

(Woodside and Dumont, 1997). All these elements represent a southward continuation of the Antalya nappes.

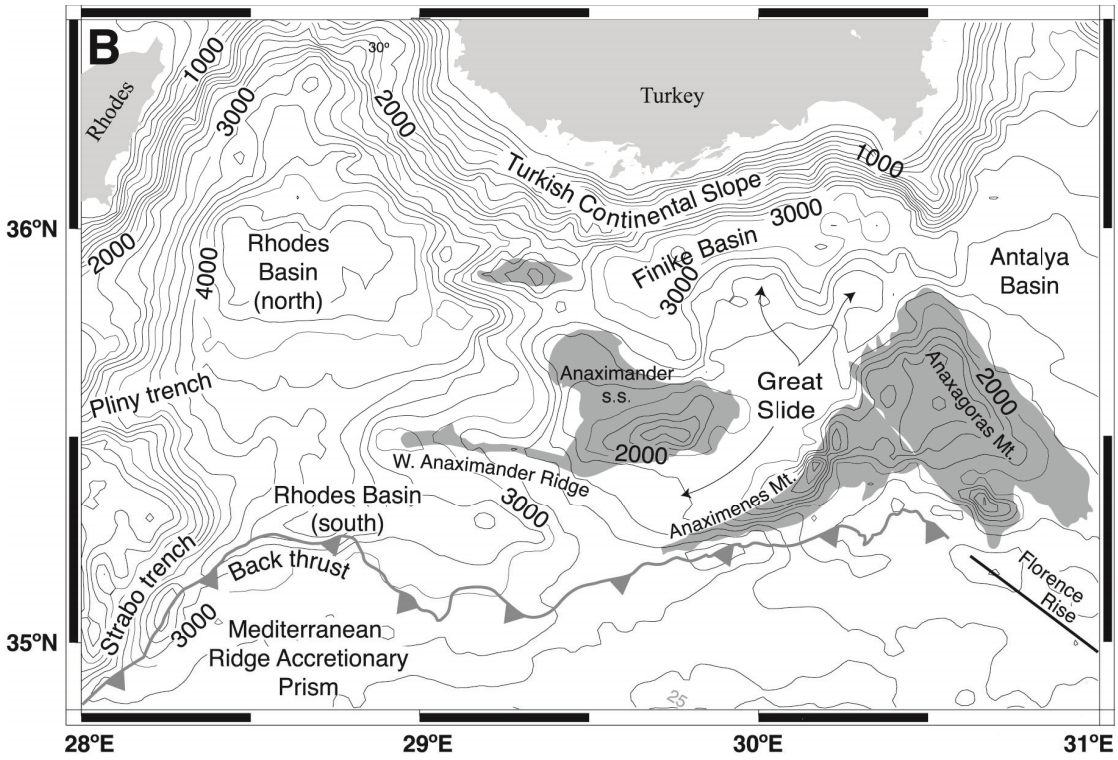

Fig. 6: Detail of the Anaximander Mountains study area with bathymetry from etopo5, made available through the National Geophysical Data Center (NDGC), with 200-m contour interval (ten Veen et al., 2004)

Messinian evaporites reach 1000 m in the eastern Mediterranean offshore of Turkey. Rollover structures associated with growth faults within the large scale turtle structures above the Messinian unconformity are a result of salt mobilization. Messinian evaporites are close to the apex of the western Mediterranean ridge and have been deposited at the backstop contact. The deeper backstop area is interpreted as the result of salt tectonics within a pre-existing fore arc basin (Chaumillon, 1995). The lower-middle Miocene deposits show a typical deep marine and flysch facies in southwest of Turkey. Plio-Quaternary sediments which were deposited in a deep marine environment, are mostly composed of siltstones, claystones, thin bedded and laminated sandstones and mudstone and there is an unconformity between the Plio-Quaternary and lower to middle Miocene flysch deposits. The thickness of the Plio-Quaternary unit is about 1500 m in Antalya offshore basin which is situated eastern of the Anaxagoras mountains and appears as a fold belt. This fold belt is represented by east-west oriented strike slip faults. Messinian-Quaternary deformation of the western part of Anaximander seamounts is characterized by right lateral strike slip faults. The eastern mountains are represented by left lateral strike slip faults and oblique faults. The mud volcanoes were discovered in the Anaximander area associated with strike-slip faults (Huguen et al., 2005). There was a change in the plate motions from north to south in the middle to Late Miocene (Dewey and Sengor, 1970). As a result of this change East Anatolian and North Anatolian transform faults developed. The extensional tectonic regime in the western Turkey increased. At the same time eastern sector of the Hellenic and Cyprus zones became more transpressive and the subduction area developed into two separate arcs resulted in the tearing of the African plate (Dewey and Sengor, 1970).

3 Cruise Narrative

(G. Bohrmann and G. Meinecke)

The R/V POSEIDON sailed from passenger terminal of Alsancak harbour in Izmir, Turkey (Fig. 7) at 09:00 am on Thursday, November 31 to perform its research mission number 462 to the area of the Anaximander Mountains, which is part of the Mediterranean Sea. The submarine Anaximander Mountains are located about 75 nautical miles south of Antalya at the Turkish coast. The area (Fig. 8) is situated at the intersection between the Cyprus Arc in the East and the Hellenic Arc in the West. Both arcs represent elements within the zone of African convergence in the South against Europe /Anatolian Plate in the North.

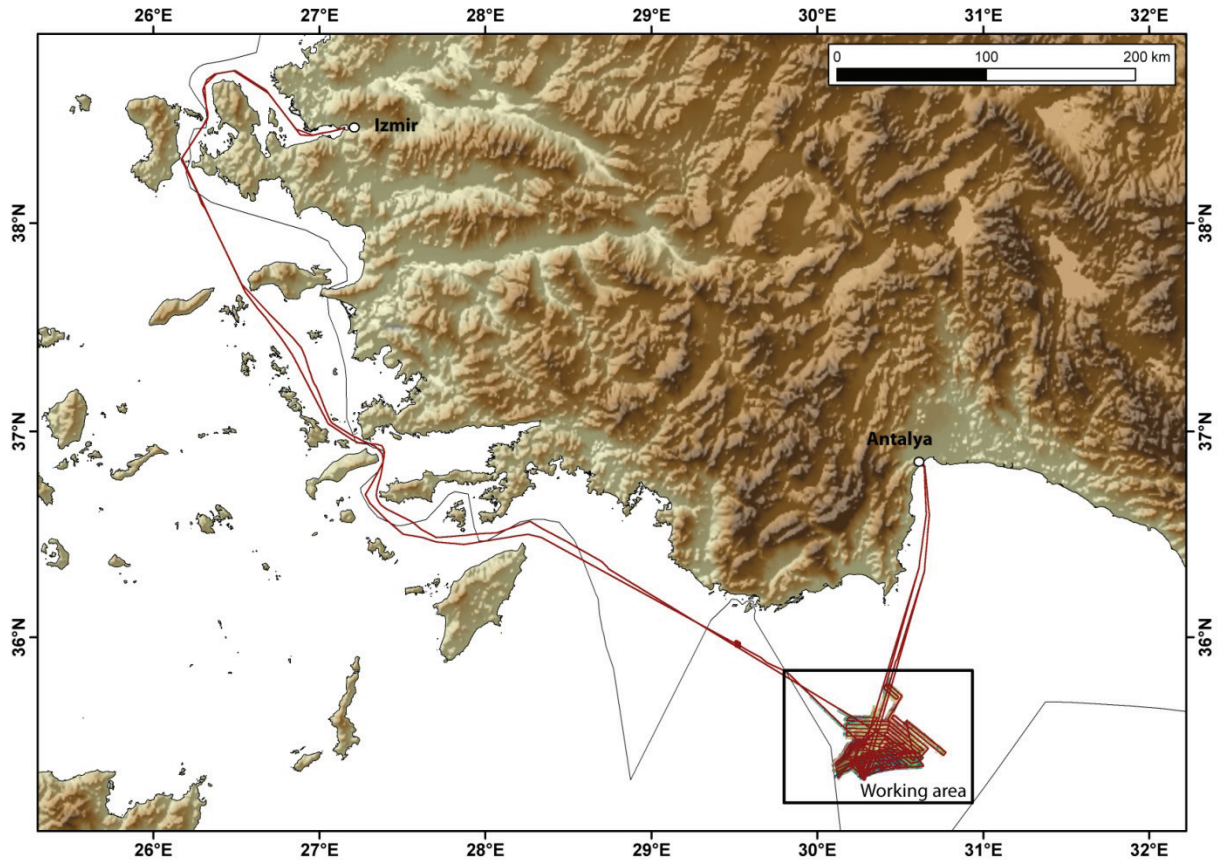

Fig. 7: Cruise track of R/V POSEIDON cruise 462 with harbour stops in Izmir and Antalya; area of research is shown by the box (see Fig. 8). The thin line marks the border between Turkey and Greece.

From the tectonic point of view the Anaximander Mountains represent a complicated structure dominated by sinistral strike-slip faults (Zitter et al., 2005). Within the frame of this compressive tectonic style several mud volcanoes have been developed, whereas not only mud but also fluids and gas emanation from the sea floor are found. Those active emissions from the sea floor are a global phenomenon and are interdisciplinarily analysed by the DFG Research Center and Cluster of Excellence MARUM in the frame of research area “geosphere biosphere interaction”. Here the main interests are gas emission sites, where methane bubbles ascent from the sea floor into the water column. It is known from other sites that those bubbles emanating from the sea floor within the gas hydrate stability zone are protected by thin gas hydrate skins from being dissolved in the sea water. Those emissions of gas bubbles from the sea floor within the gas hydrate stability zone are always associated with near-sea floor gas hydrate deposits. Up to now, gas hydrates in the Eastern

Mediterranean are only known from the Anaximander area, which can be explained by the absence of Messinian evaporites here because saline water or brines are changing the stability field of hydrates to lower depths. Gas emissions from mud volcanoes could be proven during R/V METEOR M70/3 for the first time in the Anaximander Mountains (Bohrmann et al. 2008). During P462 we used the SEABEAM 3050 system to document further gas emissions and to sample shallow gas hydrates related to the gas seeps. A further major topic was to use AUV SEAL 5000 to map micro-bathymetry of four mud volcanoes in order to plan future ROV dives for exploration of the mud volcanoes in the Anaximander area in more detail.

Coming from a transit cruise from Portimao, Portugal, R/V POSEIDON entered the harbour of Izmir in the afternoon of 27 October and stayed for three and a half days in the port of Alsancak Izmir. On Monday October 28, a welcome reception took place onboard the research vessel with high-ranked guests from policy, economy and science. Margit Häberle, the German consul general in Izmir, master Matthias Günther and Prof. Dr. Gerhard Bohrmann (chief scientist and representative of the University of Bremen) invited to the event onboard R/V POSEIDON. The reception was excellently prepared by the German consulate general and the shipping company Briese and the event on board R/V POSEIDON was a great experience. During the further port call the scientific crew and the scientific tools had been brought on board, in total 4 containers were unloaded and the labs have been installed. Eleven scientists from Germany and Turkey embarked on 28, 29 and 30 October. On Wednesday, 30 October a group of scientists and students from the Institute of Marine Sciences and Technology of the Dokuz Eylul University in Izmir accompanied by a film team of the national TV channel visited the vessel and discussed possible options for future cooperation in marine science.

After two days transit through the Aegean Islands along the border of Turkey and Greece (Fig. 7) we reached the area of investigation on Saturday morning, 2 November. In the night before the new motion sensor for correcting the multibeam system was calibrated in the area of the Antalya basin. On Thessaloniki Mud Volcano (TMV) a first attempt to launch an AUV dive failed and we performed during the day a detailed multibeam survey and a CTD station on the TMV in order to develop a new velocity model for the water column. The velocity model is a prerequisite for getting adequate depth information from the multibeam. Since one of our Turkish observer had a problem to stay on board we decided to steam in the night to Antalya where we disembarked the cruise participant in the morning of Sunday, 3 October. The way back from Antalya to the working area was used to enlarge our multibeam mapping area specifically to map the shallower parts of the Anaximander area with the SEABEAM 3050 from ELAC Nautik installed on board R/V POSEIDON.

On Monday, 4 November a series of gravity cores and a DAPC core were taken at TMV. For sampling we took 2 sites on top of the mud volcano and 2 locations at the eastern flank, where high backscatter intensities and gas flares have been observed in records of past cruises. Flare mapping of the area showed that gas emission sites exist on the eastern and south-eastern flanks of TMV, probably related to an N/S tending fault zone. In these cores only mud breccia from the top of TMV contained traces of gas hydrates. The flare site east of the TMV seems to be covered by seep carbonates which have been sampled together with chemosynthetic fauna, mostly lucinid bivalves. After a night program of multibeam mapping a further DAPC was deployed on TMV during the following Tuesday, 5 November and the AUV SEAL 5000 did a large mapping survey (AUV Dive 54) of the TMV overnight. The survey covered an area of more than 6 km^2, from which the main mud

volcanic structure, around 1 km^2, showed a sequence of piled up layers with two main eruption centers and some smaller parasitic mud emission sites.

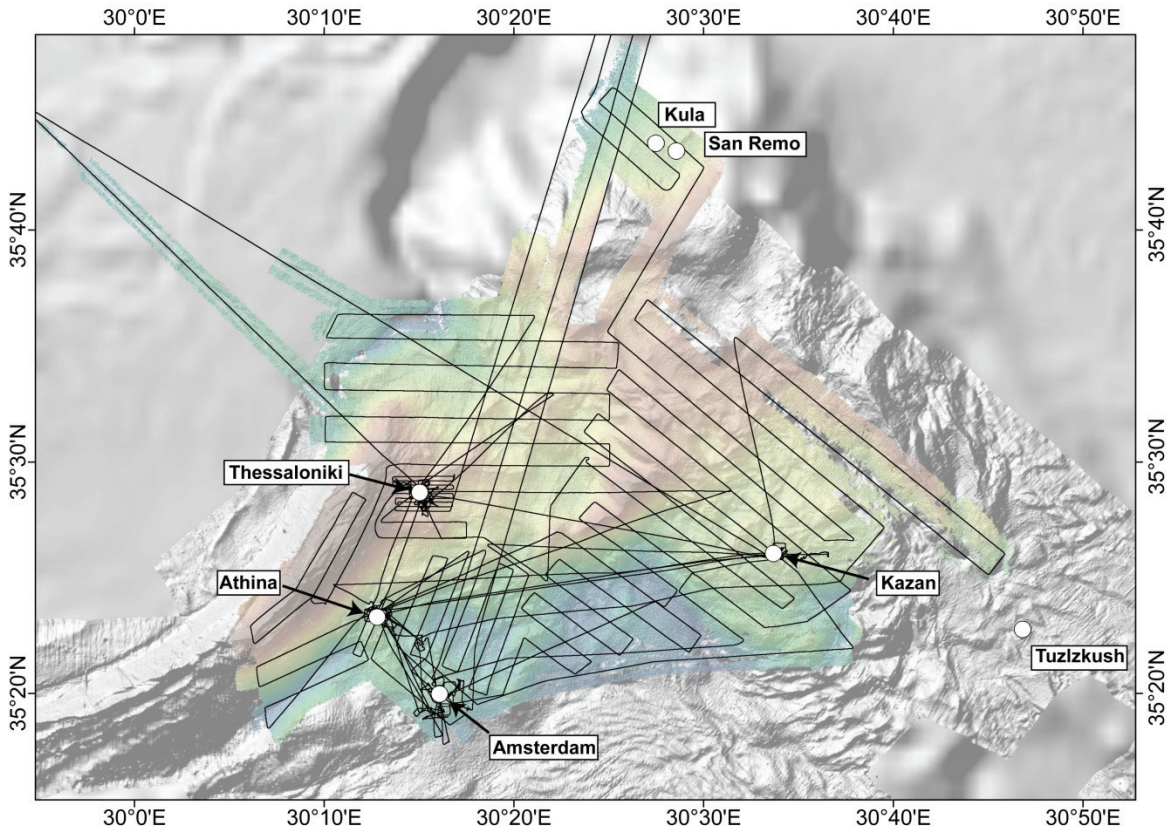

Fig. 8: Cruise track of R/V POSEIDON cruise 462 in the area of the submarine Anaximander Mountains. The main mud volcanoes are shown.

During Wednesday, 6 November the weather became bad, and during wind speeds of Beaufort up to 7 the AUV dive was cancelled. After a DAPC deployment we performed further mapping tracks with the hull-mounted multibeam. On Thursday, 7 November we took seven gravity cores on and around TMV at positions we carefully worked out on the basis of the new AUV micro-bathymetry map. Beside some seep carbonates and chemosynthic animals like clams and tube worms on high backscatter patches and gas emission sites outside the main mound of TMV, we also sampled the different mud pie patches. All sediment cores from there recovered mud breccia in the lower parts and it seems that depending on the age of the mud flows various thick pelagic sediments are overlying the mud flows. Despite bad weather conditions further mapping in the night was still possible and we could enlarge the coverage of the new multibeam data.

On Friday, 8 November we took 4 gravity cores on the oval shaped plateau of Kazan Mud Volcano (KMV) and sampled diverse mud breccia yielding different amounts but generally very small amounts of gas hydrate. From late afternoon to the morning of the following day (Saturday, 9 November) AUV SEAL dived on KMV (AUV Dive 55) to perform the micro-bathymetric measurements. KMV is an isolated oval shaped hill with a relative flat plateau above the 1700 m contour line. Mud flows from this top seem to have been moved to both sides to the west and to the east and changed downhill the direction to the south. The backscatter of the older multibeam map showed that these mud flows are covering a large area downhill to the southern direction. Unfortunately the AUV stopped in the middle of the dive, because of a malfunction command and came back to the surface guided by

its own backup program. The AUV Dive 56 ended earlier, so that only the upper part in the centre of KMV was mapped. The new map from the night already guided us to do more sampling close to the area, where we thought there is the center of the mud eruption, and on Sunday, 10 November we took 3 more cores (2 gravity cores and one DAPC). Although in all cases mud breccia was sampled, the presence of gas hydrate was found very rarely.

At the evening of Sunday, 10 November AUV Dive 57 started on Athina Mud Volcano (AthMV) and was performed the entire night until the AUV was recovered in the morning of 11 November. The newly measured micro-bathymetry showed the complicated seafloor topography with steep slopes and downward mud flows over a very broad surface of the flank of the mud volcano. The ring-shaped crater structure of more than 1 km in diameter is characterized by two elevations which are both seen in the AUV map with steep scarps of around 20 m in height, most probably evolved by down-sag movements in the crater due to mass deficiency in the deeper part of the volcano. Between those two scarps a relatively fresh mud flow with wrinkled surface is covering the seafloor which clearly shows a mud expulsion site in the north-eastern corner. After the dive we deployed a DAPC on KMV close to the potential mud emission outcrop and a gravity corer above a high backscatter anomaly east of the volcano. A further gravity corer sampled a prominent mud flow on the western side of the volcano, which we stored in a plastic liner for future investigation of the mud flow and the overlying pelagic sediments.

On Monday evening we started to continue mapping on Amsterdam Mud Volcano (AMV) during Dive 58 which was in small parts already done during MARIA S. MERIAN cruise M13/4 in 2009. Although the central of the AMV was already covered we planned to map more details of the rim and the southern and eastern flanks of the mud volcano. The first of several dives on that very large structure covered the western central part of the mud volcano.

After recovery of AUV SEAL on Tuesday, 12 November, we deployed three gravity cores on AthMV from which two cores sampled sediments at distinct gas emission sites observed in the AUV water column data from the dive on that mud volcano. The third gravity corer was deployed directly at the extrusion centre of the mud volcano on top of the structure. This location was not known before the AUV mapping and showed the structure in great detail. The retrieved sediments degassed a lot and the remaining result showed up in very fluidized or soupy mud breccia, which is a typical indication for former existed gas hydrates in the sediments. Unfortunately these hydrates decomposed already during their transport through the warm water column. In the following we deployed a DAPC at the same site to sample the hydrate-bearing sediments, however the pilot corer could not release the penetration of the piston corer and corer and autoclave remained without any sediment. A mapping program during the night added more lines of multibeam measurements to the southern part of the research area.

On Wednesday, 13 November, in the morning we deployed the AUV (Dive 59) in order to map the missing eastern part of the Amsterdam Mud Volcano. This mission took the whole day until early evening. At 21:00 we recovered the AUV, which performed successfully the complete mission of Dive 59 and we left the working area directly afterwards heading towards Antalya.

On Thursday morning, 14 November, we arrived in Antalya harbour. Main purpose of this stop was a crew change from scientific personnel. Three persons left the vessel and 3 new scientific crew members stepped in for the second leg.

On Friday, 15 November, we left Antalya, heading to Amsterdam Mud Volcano, again. We arrived in late evening and run a CTD cast. Main purpose of the operation was the calibration routine of the temperature probes, necessary to run the heatflow probe, envisaged for the next day. In addition, an acoustic releaser was tested as well. During night a SeaBeam survey was performed at Anaximander survey area.

On Saturday morning, 16 November, we re-run a CTD cast at Athina Mud Volcano, due to not successfully operated releaser during the first CTD cast. Afterwards we started to operate the heatflow probe. During station HF1 until HF5 we measured a heatflow profile down the Athina crater, starting on top at the assumed crater center. Hereby following temperature gradients have been observed HF1: 80°C/km, HF2: 50°C/km, HF3: 30°C/km, HF4: 50°C/km, HF5: 26°C/km. In the evening we deployed the AUV again for Dive 60 at Amsterdam Mud Volcano.

On Sunday morning, 17 November, we recovered the AUV after complete mission duration. During Dive 60 the missing southern area of Amsterdam Mud Volcano was mapped successfully. Afterwards, we had to re-run the CTD cast, due to not well calibrated temperature probes during first CTD cast. During calculation of temperature calibration we run a SeaBeam profile, ending at Athina Mud Volcano. In the late afternoon we prepared the next AUV dive. Dive 61 focused on the missing map areas on the southern flank of Athina Mud Volcano and a distinct area at the base of mud volcano, potentially a newly evolved small mud volcano.

On Monday morning, 18 November, we recovered the AUV after successful mission at AthMV. Afterwards, a second heatflow probe profile was performed on Athina Mud Volcano, station HF-6 until HF-9 starting on top and going down slope. Results of temperature gradients are not calculated, yet. After termination of heatflow measurements we shifted location to Amsterdam Mud Volcano and run two gravity cores at mud volcano site. At both locations, no gas hydrates have been observed. Due to changing weather conditions, we had to cancel the envisaged AUV Dive 62 for the night. Instead, we run a SeaBeam survey of the western part of Anaximander working area, ending at Kazan Mud Volcano.

On Tuesday, 19 November, we started a heatflow probe survey at Kazan Mud Volcano, running sampling station HF-10 until HF-16. The profile was planned to survey along the N-S going crest of central Kazan Mud Volcano area. Results of temperature gradients are not calculated, yet. At noon the profile was finalized and we had to shut down station work of P462 cruise and started our 40 hours transit back to Izmir.

On Thursday morning, 21 November, we reached Izmir harbour where we had to terminate the R/V POSEIDON 462 field cruise campaign; unloading of scientific equipment was started and terminated at evening.

4 Multibeam Work

Multibeam data were collected and processed from both: the vessel installed ELAC system and the AUV-based Reson multibeam.

4.1 Bathymetric Mapping

(C. Ferreira)

At cruise P462 multibeam surveys were made using the multibeam echosounder (MBES) available at R/V POSEIDON. The system is from ELAC NAUTIK. It is a 1.5-by-2-degree mid-water MBES operating with a frequency of 50 kHz and a maximum number of beams of 384. This equipment is designed for mapping until 3000 meters depth but due to unknown reasons (perhaps ship noise or something else) the maximum range we could achieve was around 2000 m. The maximum swath coverage at the depth ranges between 1200 and 2000 m was of around 1 (or 2 at the shallow parts) time the water depth. But this is in agreement with the official performance calculations done by ELAC.

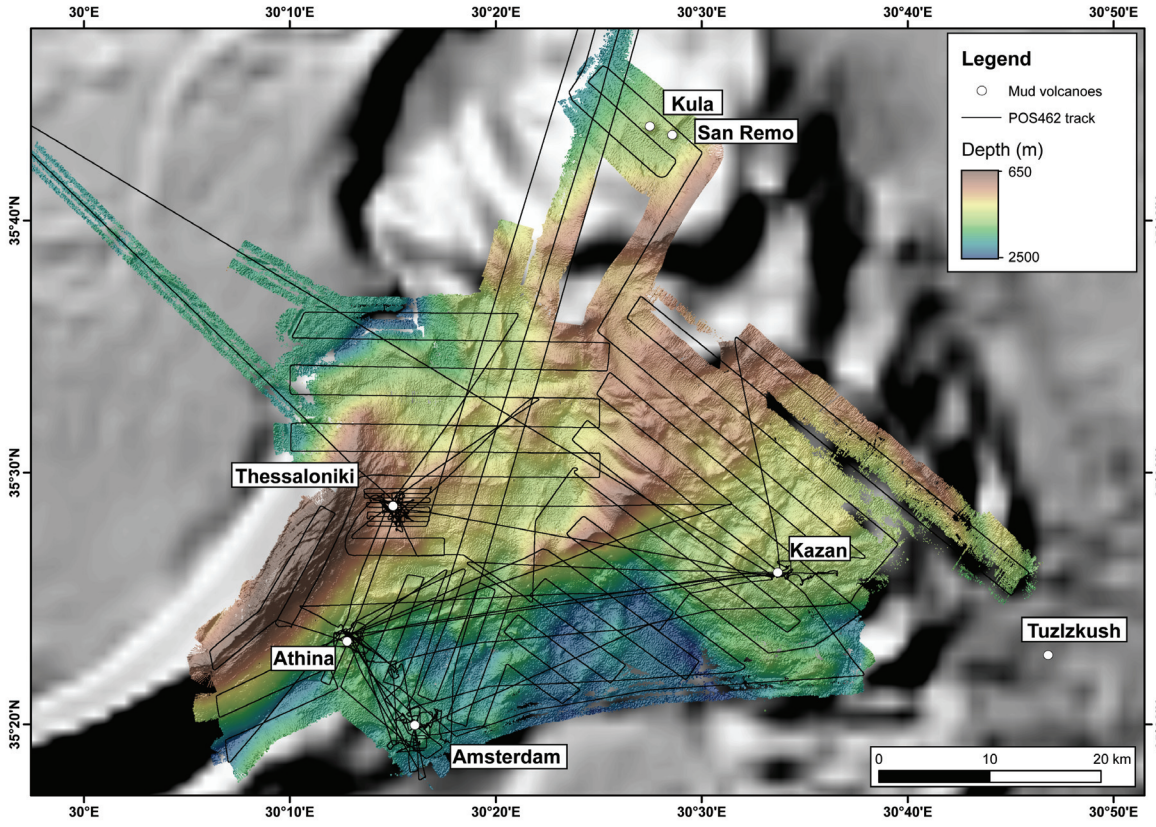

Fig. 9: Overview map showing the survey lines conducted during P462 and the resulting bathymetric grid produced.

All surveys done using the Seabeam 3050 were designed for bathymetry acquisition and/or bubble mapping (AKA, water column imaging). However, the 2000 meters range as mentioned before, limited us. Another limitation is the way in which the Seabeam 3050 system handles the beam-steering. Not like Kongsberg, the ELAC system has static beam positions/angles, and therefore we suffered from a beams reduction that varied according depth. At depths around 1200-1400 meters the maximum number of beams was around 180-160 beams, and at the deepest parts (1800-2000 meters) the maximum number was around 140-120 beams.

The data acquisition was done using the Hydrostar software from ELAC. This program registers data using the XSE format, which is also created/maintained by ELAC. No data was recorded with HYPACK due to the bigger files size (since this software stores the data in ASCII format instead of binary, and because of a very well-known bug regarding the files that cross the midnight hour).

At the cruise maps were produced daily using the post-processed data made onboard. During this fast post-processing, the multibeam data were analyzed using the latest MB System 5.4. revision 2157 (Caress and Chayes, 2001). Therefore the post-processing tool onboard (HYPACK) was never used.

The cruise was not without problems. The navigation and motion sensor CODA F180 self-calibration was not successful after 36 hours. And even after the 3 weeks duration of this cruise the system was still trying to calibrate itself. The possible reasons for that are discussed in the chapter below. A quick explanation here is that the setup of this system is incorrect. The F180 presented sometimes severe heading problems, which manifested as a heading offset around 20-30 degrees for periods of half an hour. Another less critical issue was the lever arms inserted into Hydrostar, HYPACK and the F180 are left as zero for the recalculation of the motion at the sonar head position (AKA, the transducer from the multibeam). This is an unfortunate mistake also present inside the official documentation for the Seabeam 3050 onboard R/V POSEIDON, but which we could solve applying these offsets on post-processing. The person responsible for these two systems must address both issues.

Problems with setup and calibration of the F180

During the cruise P462 we performed the calibration procedure for the INS F180 from R/V POSEIDON. The reason was a non-static offset for the heading between this sensor and the heading from the vessel's gyro. Normally this procedure is supposed to take between half an hour and two hours. This one took thirty-six hours and the F180 system was still trying to autocalibrate itself. Therefore we aborted the procedure since we had to continue with the other (scientific) activities for the cruise.

However, one thing called our attention, for the last hour of the F180's heading calibration the heading offset between the F180 and the gyro stabilized at an almost constant offset around 1.75 degrees. And according to multibeam specialist Christian Ferreira from MARUM (and who has been participating in several system calibrations (INS and multibeam) on R/V METEOR, M.S.MERIAN and HEINCKE), this offset could be due to the fact that the angular offsets at the F180 were left empty (with zero values). So on Fig. 10 the official setup values are shown mentioned by ELAC Nautik as the official values for the F180 setup:

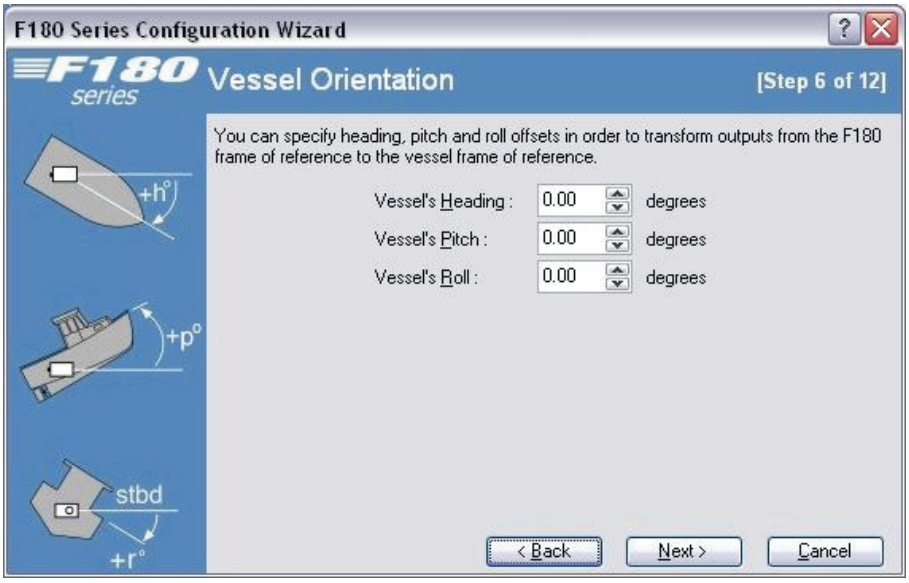

Fig. 10: The heading (and roll/pitch) offsets were left as zero.

However, the offsets measured by survey company Overath & Sand clearly show different non-zero values for these angular offsets (Fig. 11):

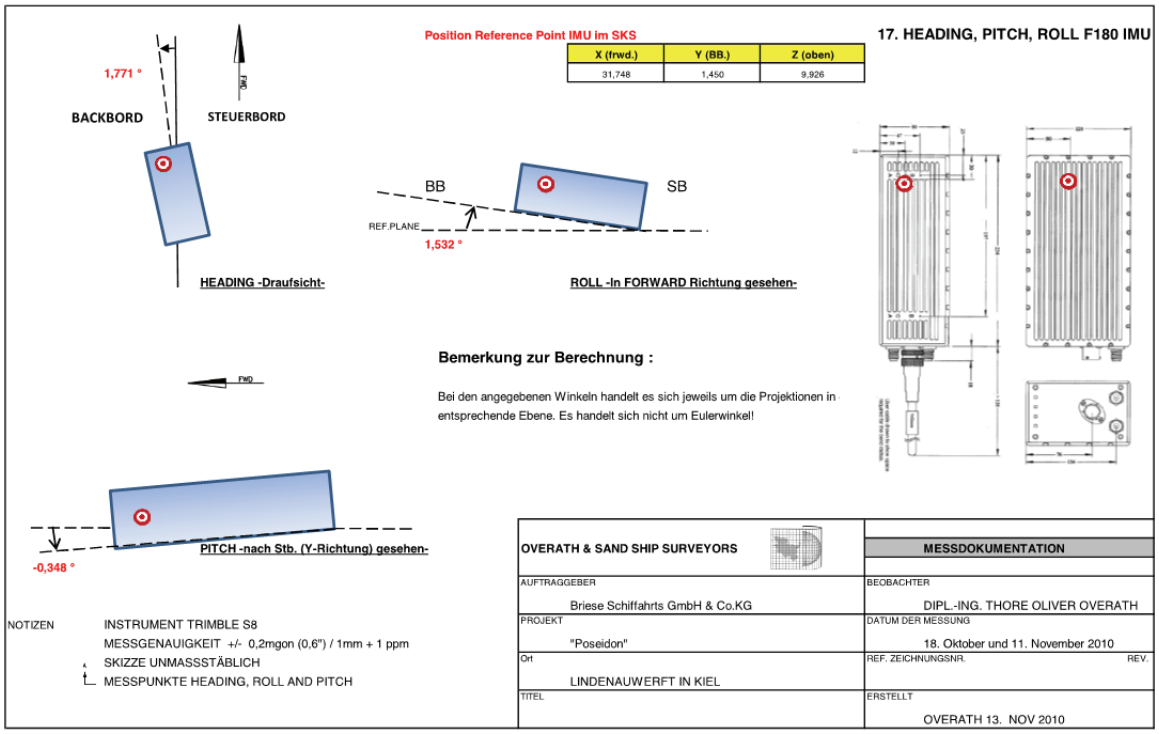

Fig. 11: The real heading (and roll/pitch) measured by the survey company Overath & Sand.

So the heading offset between the gyro and the F180 is due to the fact that the values measured by Overath & Sand are not inserted into the setup of the system. This incorrect configuration was probably the reason why the F180 never really finished the system self-calibration after 7 hours performing “8” shaped survey lines.

Operation of the F180

During the multibeam surveys several occasions were observed where the heading sent by the F180 to the ELAC Seabeam 3050 contained errors. The problem occurred as an error of the heading around 25-30 degrees that happened for around half an hour and then suddenly went back to the normal offset of 1.7 degree (between F180 and Gyro). The screenshot from the post-processing software for multibeam data MB-System illustrates the problem:

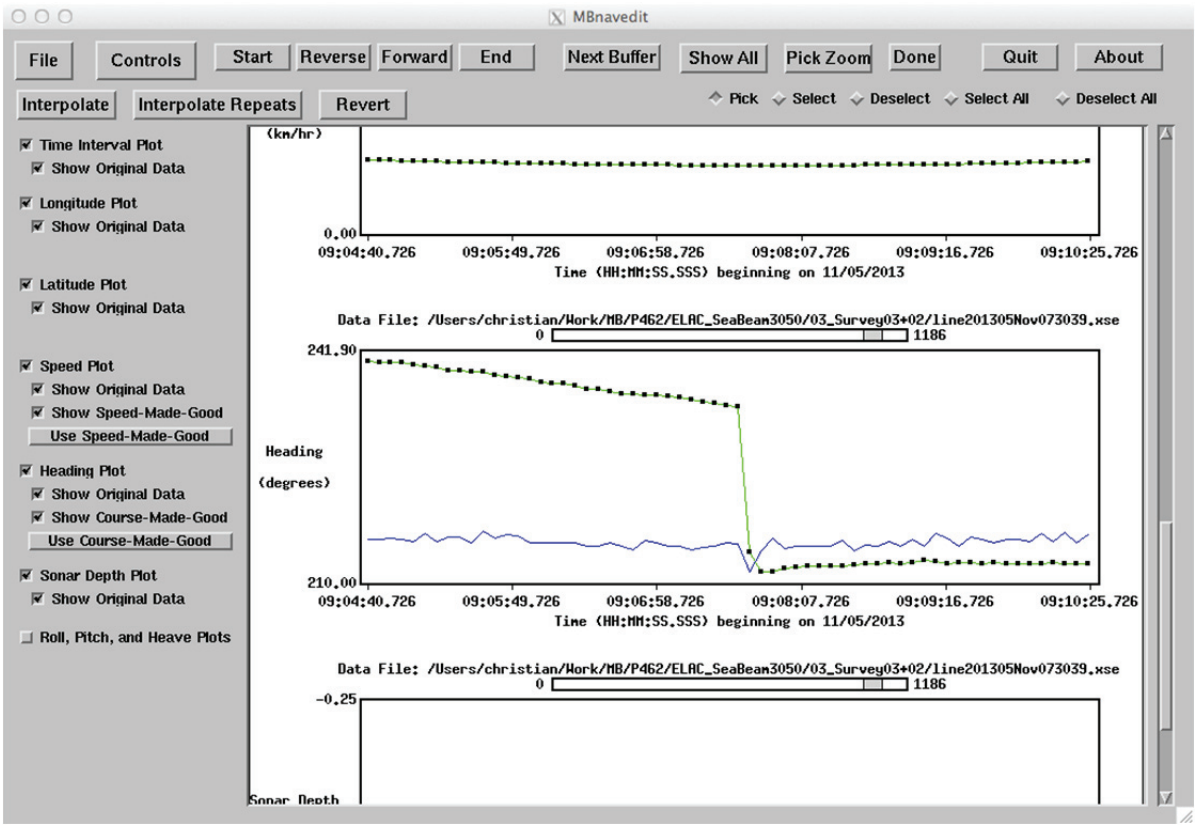

Fig. 12: The navigation editor from MB-System showing the heading error. On the left are the wrong heading values (the dotted line showing a decay). On the right side are the correct heading values and characterized by the stable green dotted line, and in between a jump of around 25 degrees.

It seems that for some reason the F180 lost completely the heading calibration and slowly tried to go back towards the correct value (illustrated by the decay seen in the heading values of the left side of the line). However it's more astonishing that suddenly the system goes back to the correct heading (but still with the static offset of 1.75 degree).

The next screenshot (Fig. 13) shows the exact same heading jump but this using the grid viewer (left side) and the sounding editor (right side) from MB-System.

It is inexplicable why the heading jumps off by 30 degrees, and also why/when/how it jumps back to the correct value. So the reason(s) for these heading jumps remained still unknown after the P462 cruise, and it is recommended by the scientists that the F180 system should be sent for further investigation to the manufacturer (CODA). This kind of bad system performance cannot be accepted since it impacts significantly the accuracy and performance of the data collected by the multibeam system.

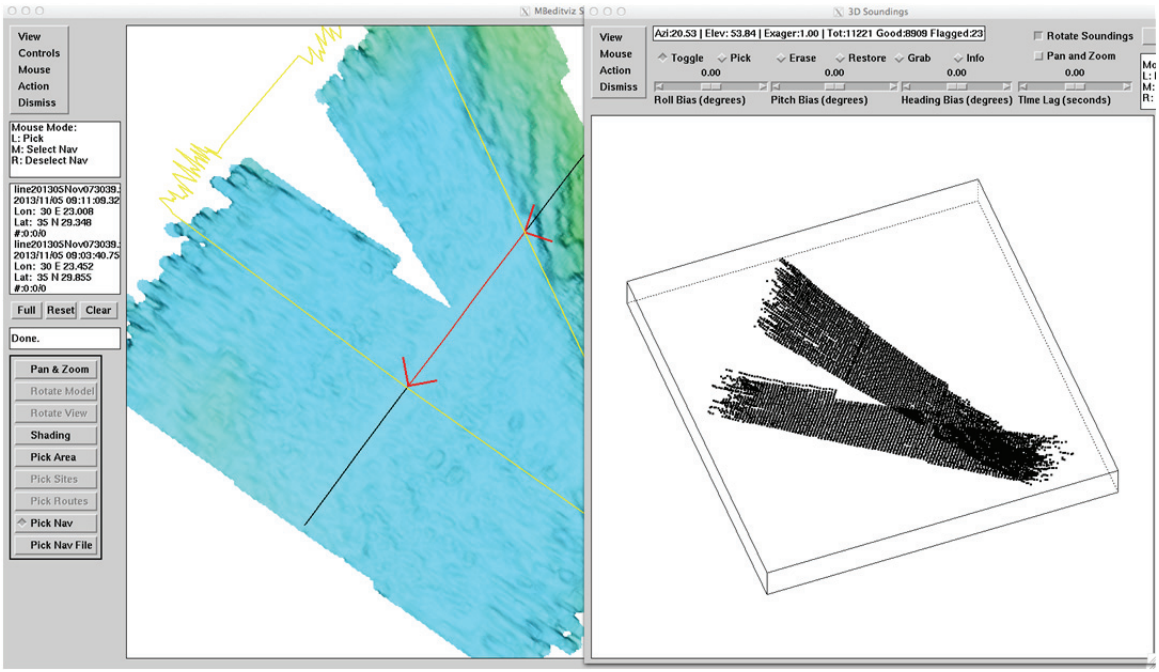

Fig. 13: A screenshot from MB-System showing the moment when the heading from F180 jumps back the correct value.

Setup from HYPACK and ELAC Hydrostar

So the offset for the heading between the vessel frame and the F180 frame were also 1.7 degrees. Of course this value could be applied at other places like HYPACK and ELAC Hydrostar. However, on the existing documentation produced by ELAC (see document "How to setup the multibeam onboard R/V POSEIDON SEABEAM 3050 Series") all places where this offset could have been applied were left as zero or the information was omitted (see Figs. 14 to 16):

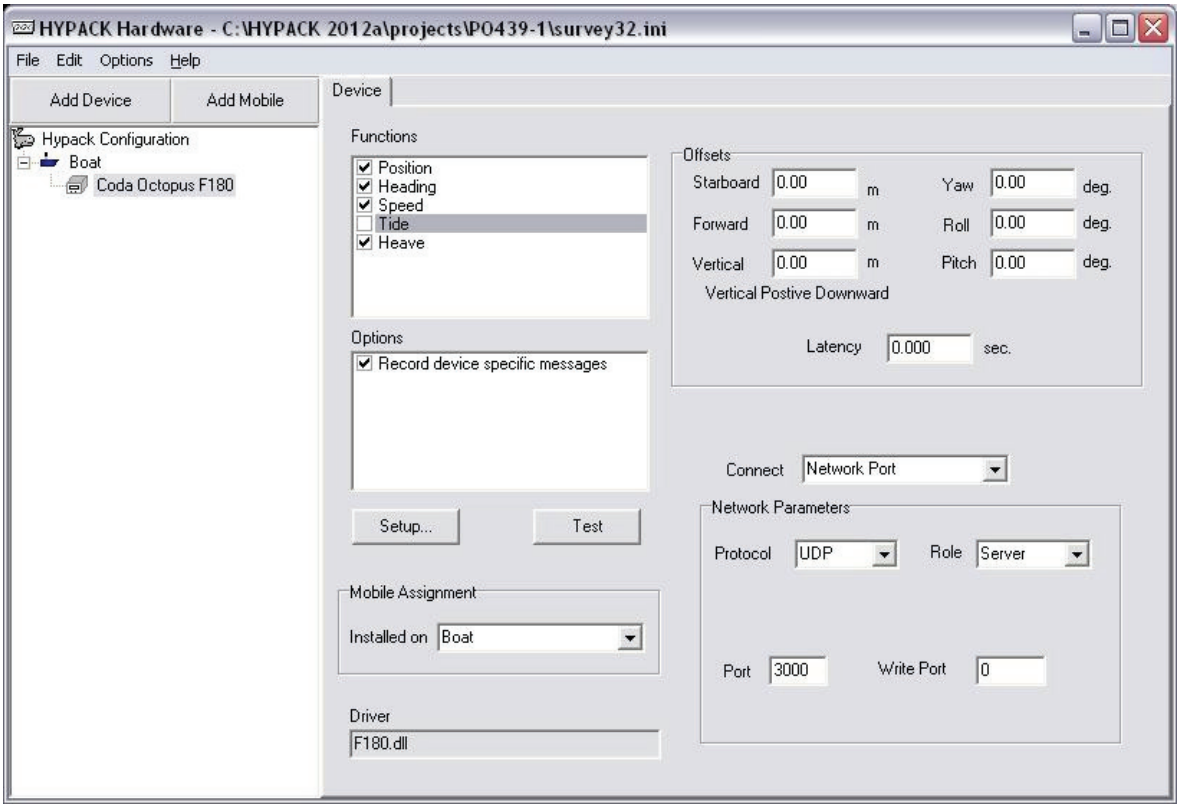

Fig. 14: Offsets inserted into the F180 driver inside HYPACK hardware.

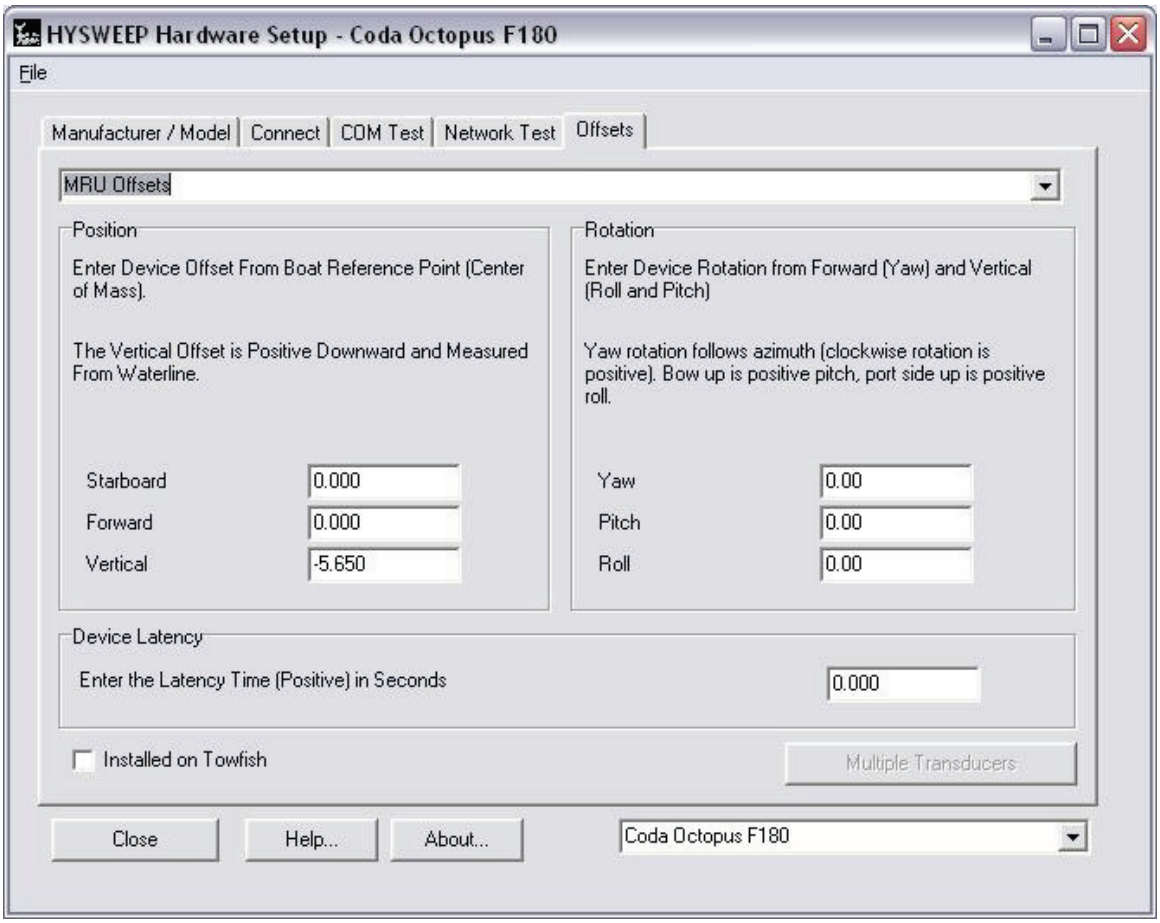

Fig. 15: Offsets inserted into the F180 driver inside HYPACK hardware driver setup.

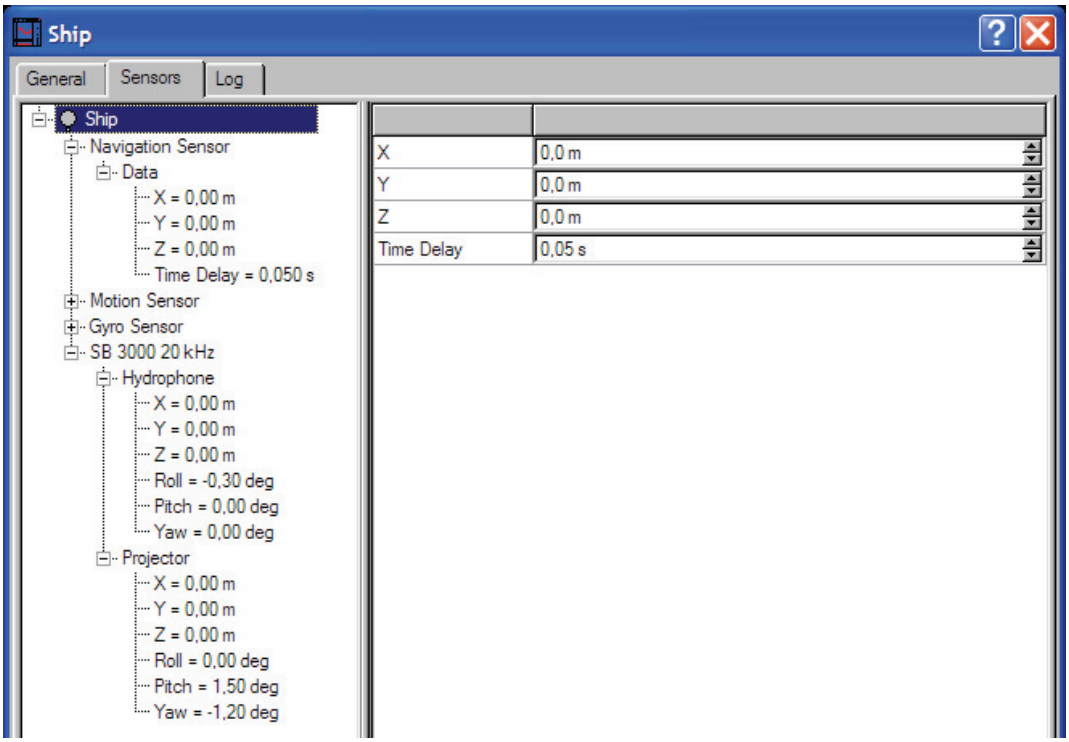

Fig. 16: The values for angular offsets of the F180 could also be inserted into the "motion sensor" (roll/pitch) and "gyro" (for the heading), but here they are not visible. However, existing pre-defined template projects for the ELAC Hydrostar at R/V POSEIDON also show the gyro offset as zero.

4.2 Water Column Imaging

(M. Roemer)

From the seafloor emanating gas bubbles can be visualized with multibeam echosounder systems due to the high impedance contrast between free gas and the surrounding water, producing a high backscatter signal in the water column data. Gas emissions visible in echograms are commonly called flares. The only condition, the multibeam systems need to provide, is that all beam information including the water column is stored and recording is not restricted to the seafloor depths. The ELAC multibeam mounted on R/V POSEIDON (Seabeam 3050) fulfills this condition and could therefore be used for the purpose of flare imaging during P462. Flare mapping with the ELAC system was unfortunately limited by the water depth and resolution. Below ~1600 m water depth it became almost impossible to detect flares, especially when not very intense. The background noise increased with depth and reached in ~1600 m approximately the same backscatter intensity as flares, with the effect that possibly existent flares were probably masked (see Figs. 17 and 18). Besides Thessaloniki MV all other mud volcanoes investigated during the cruise are located deeper than 1600 mbsl and reliable data could not be achieved. In those areas we could use the multibeam data recorded by the AUV for flare mapping, moreover with a much higher resolution.

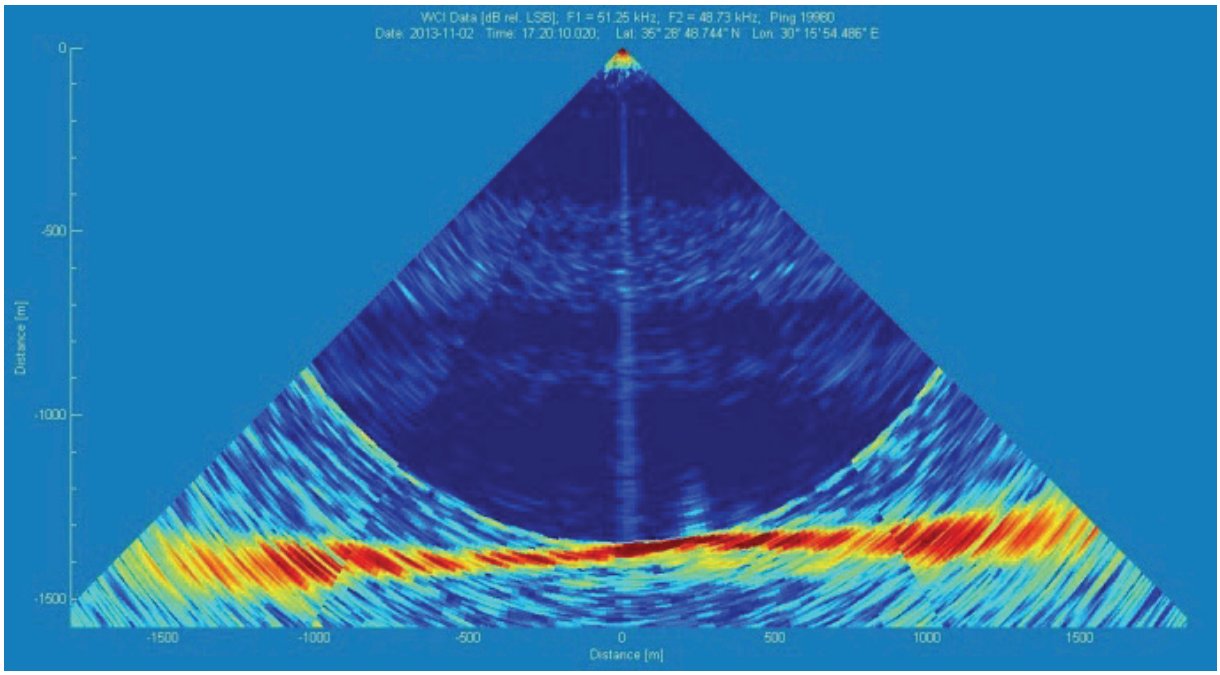

Fig. 17: Swath echogram example recorded in about 1200 m water depth. Approximately 100 m on starboard side is a flare of ~100 m height visible.

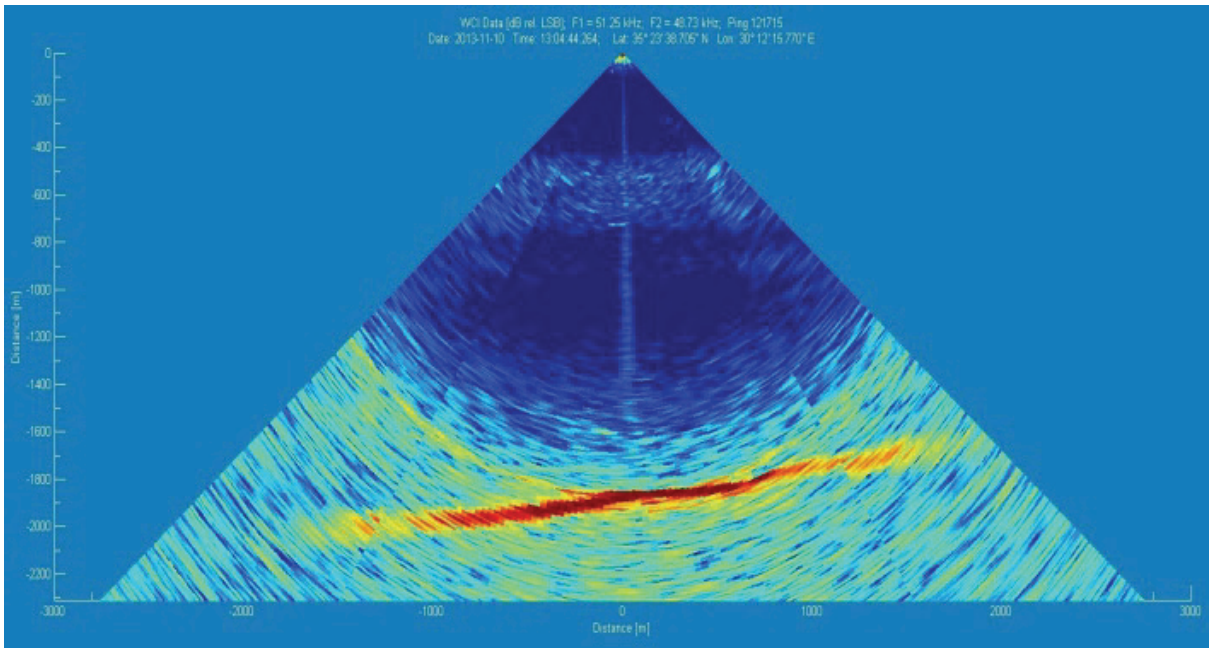

Fig. 18: Swath echogram example recorded in about 1800 m water depth. Strong noise impedes the detection of flares.

4.2.1 ELAC Water Column Archiver and Viewer (ship based multibeam)

In order to archive, visualize and analyze the water column data of the ship-based multibeam system, several steps have to be performed using different software components:

1) *ELAC WCI Archiver*:
   Software to store the multibeam data including the water column information. The data is archived in *.wci files, which are collected in sub-folders including each 1024 *.wci files. A *.wci file is created after 5 seconds and has a size of about 10 – 20 MB.
2) *HydroStar WCI Viewer*:
   The online viewer enables to visualize in almost real time the swath echograms during the surveys or to replay data again after the performed surveys. Few settings can be changed to enhance the view for the best performance of flare mapping (Fig. 19). However, these changes here did not affect the raw data storage of the *.wci files.

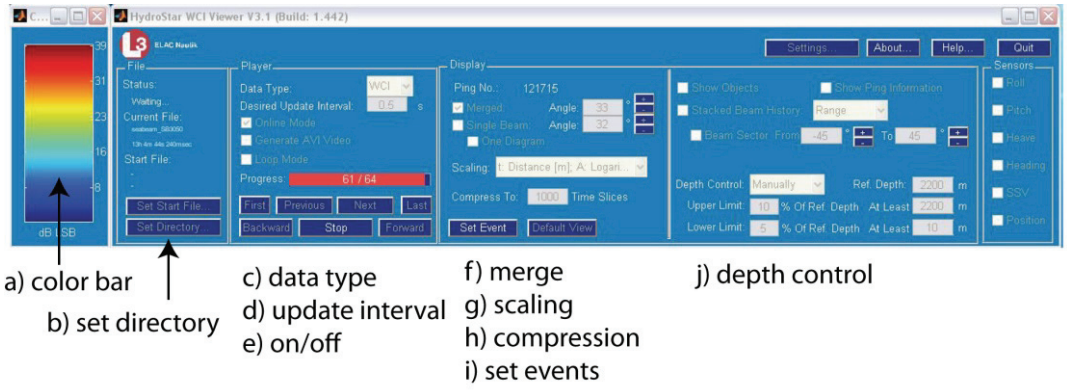

Fig. 19: Settings for the HydroStar WCI Viewer.

3) *WCI2GWC:*
The converter was created by GEOMAR (Jörg Bialas) and generates *.gwc files from the *.wci files stored through the ELAC water column archiver. We converted systematically all file-folders from the external harddrives and stored the *.gwc files on the server. A 2GB file size was chosen, which spans around 0.5 – 1 hour of survey data. For further handling this file size did not generate problems or long processing times.

4) QPS Fledermaus 7.0:
The *.gwc files can be imported to the FM Midwater software (Fig. 20) and subsequently exported as *.sd files with the command >File>Export SD>Beam Fan Time Series. The generated files can be opened in QPS Fledermaus together with grid data (Fig. 21). Using the 'select' button, the locations of flares visible in the fan can be picked from the grid and the positions exported as table or *.sd file.

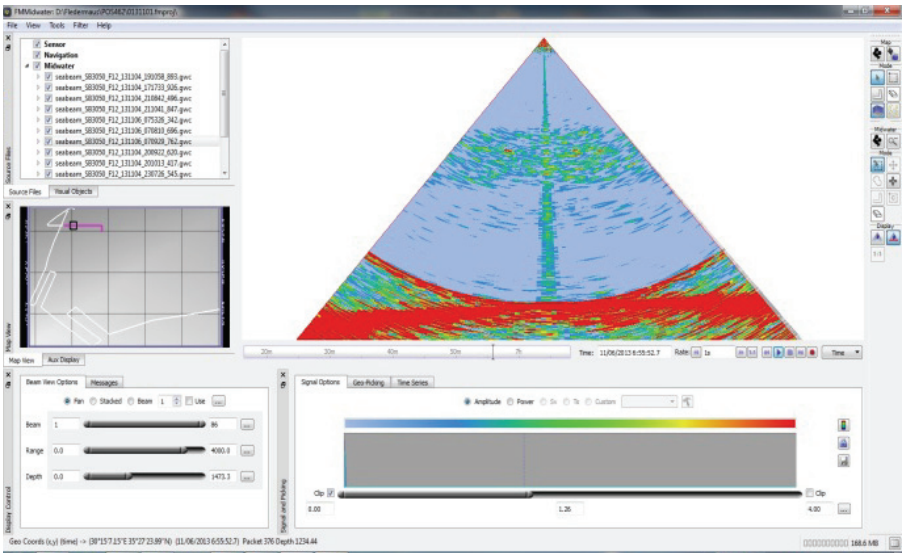

Fig. 20: Screenshot during processing with the FM Midwater software. *.gwc files can be opened and exported as *.sd files.

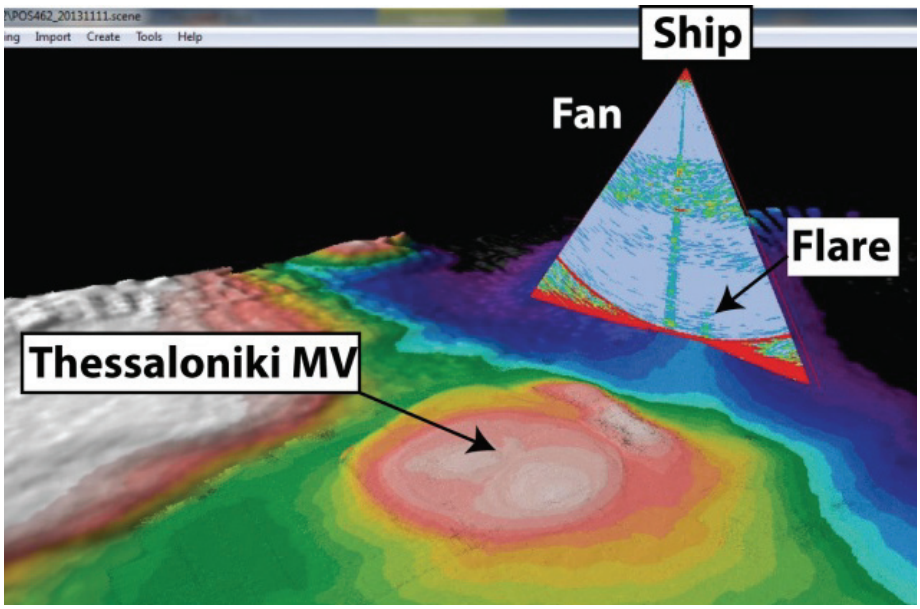

Fig. 21: Screenshot of the *.sd visualization in QPS Fledermaus.

Preliminary results from the Thessaloniki MV:

We conducted a survey of nine E-W lines over the Thessaloniki MV with a narrow line spacing of about 400 to 500 m distance in order to fully cover the area to detect flares in the water column using the ship mounted ELAC Hydrosweep echosounder. With a vessel speed of ~4kn, the survey on the 02.11.2013 lasted approximately 6.5 hours. At least 15 flares were detected (Fig. 22), whereas all flares were found to originate from the surrounding of the mud volcano but not at the center. Flares appear generally weak and have a maximum height of ~200 m. The most intense flares were detected east of the mud volcano at the crest of a small ridge structure, where about four flares are located close to each other and observed also from the two northern and southern survey lines in about 800 m distance.

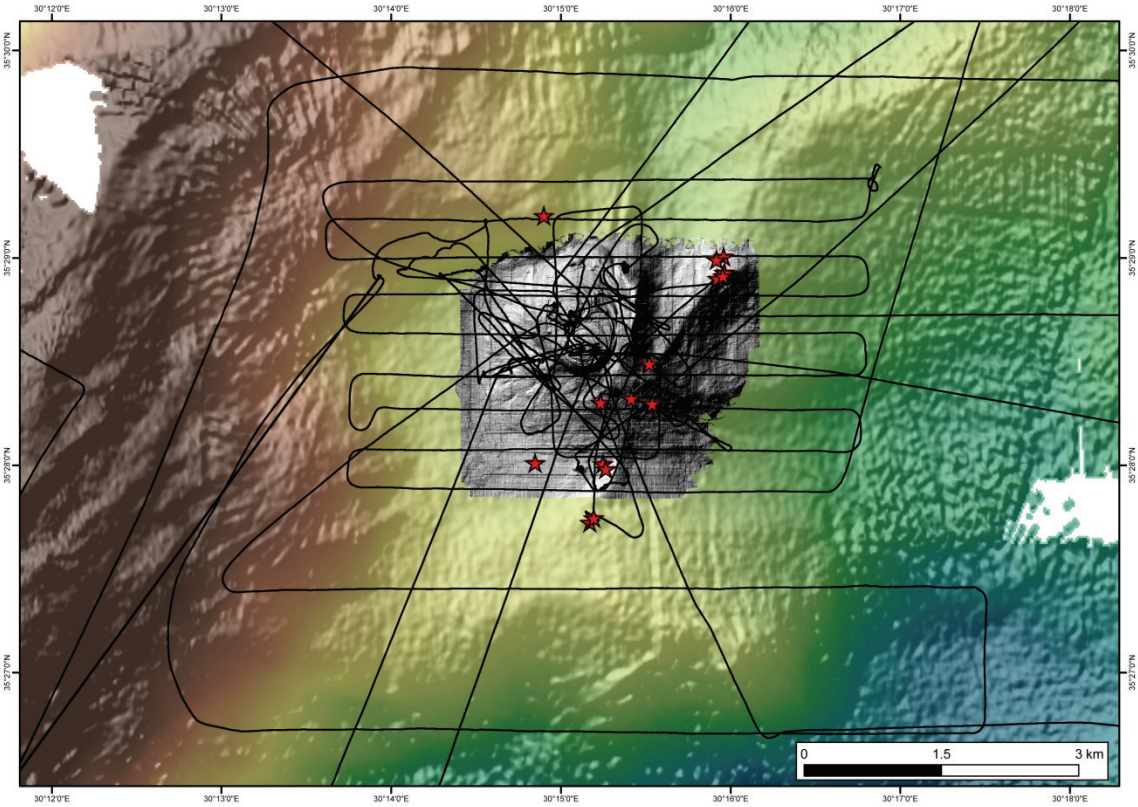

Fig. 22: Track line of survey conducted at Thessaloniki MV in order to map flares with the ship mounted ELAC Hydrosweep echosounder. Most flares (red stars) were observed east and southeast of the mud volcano structure.

4.2.2 RESON Water Column Data Analyses (AUV-based multibeam)

The multibeam data recorded with the AUV-mounted RESON MBES 7125 (400 kHz) could be used to detect and locate gas flares in high accuracy. Replaying the RAW data in *.S7k file format was done onboard with the PDS2000 software. Screenshots of each flare detected were stored and the positions at the seafloor were picked and collected in a table. Flares that were passed in the center became visible as two mirrored flares touching in the central line and the position can be determined exactly. In contrast, flares passed aside were displayed only at one side and the position was roughly picked. Further processing is needed to exactly calculate the position at the seafloor.

Thessaloniki MV: AUV Dive 54

In total, 80 flares were detected at the Thessaloniki MV during AUV Dive 54 (dots in Fig. 23). The flare distribution observed before with the ship-based multibeam system could be confirmed. Most flares were located east and south of the mud volcano structure.

Kazan MV: AUV Dive 55

During AUV Dive 55 covering the Kazan Mud Volcano we detected only four flares, which were located very close together at the northern peak of the mud volcano structure. They appear to be not very intense. Additionally, few areas east of the mud volcano show anomalies in the water column, which are not formed like distinct flares but show a cloud of disturbance, maybe produced by disperse sediments.

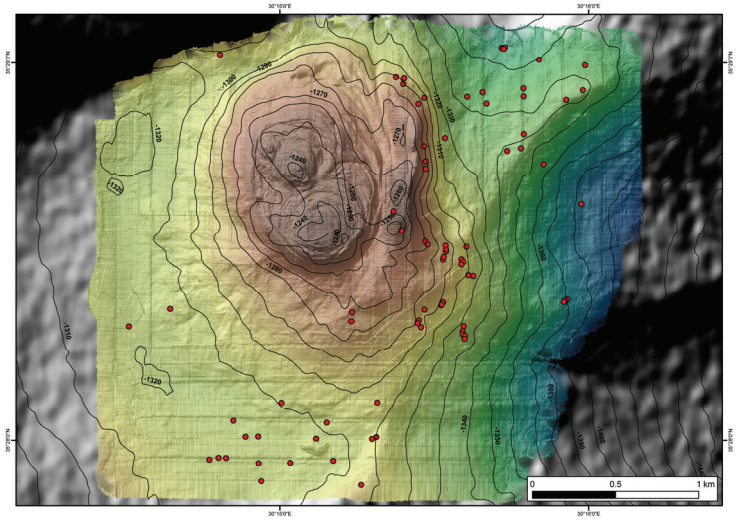

Fig. 23: AUV chart of Thessaloniki MV mapped during AUV Dive 54. Since post-processing is not completed, the data show an intermediate step of processing. Flare positions are shown by dots.

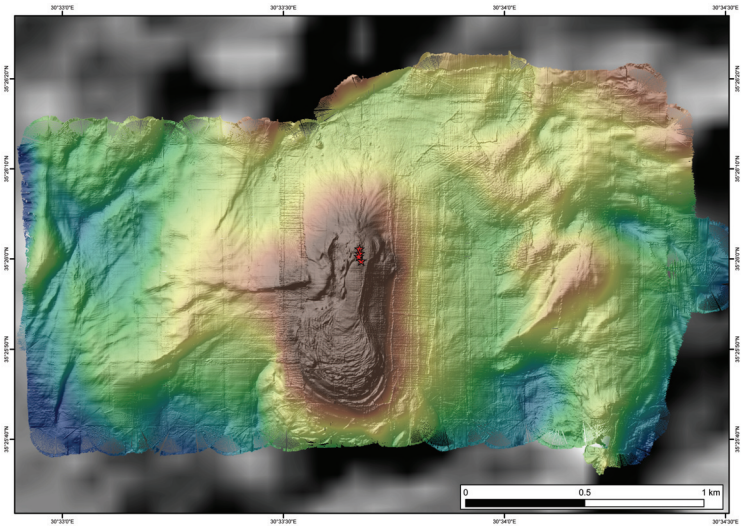

Fig. 24: Eruption center of Kazan Mud Volcano mapped during AUV Dive 55.

Athina MV and New MV: AUV Dives 56, 57 and 61

Athina Mud Volcano was mapped during three AUV dives, whereas AUV Dive 56 was cancelled after the first survey line and no flare was detected during this dive. Five flares were detected during AUV Dive 57 (Fig. 25a), interestingly not at the top of the mud volcano structure but at the eastern flank.

AUV Dive 61 was conducted to fill last gaps in the bathymetric map and to enlarge the coverage to the southwest, where only one additional weak flare was found. The last part of AUV Dive 61 was used to map the newly discovered mud volcano, where we could confirm active gas emission by recording five flares (Fig. 25a).

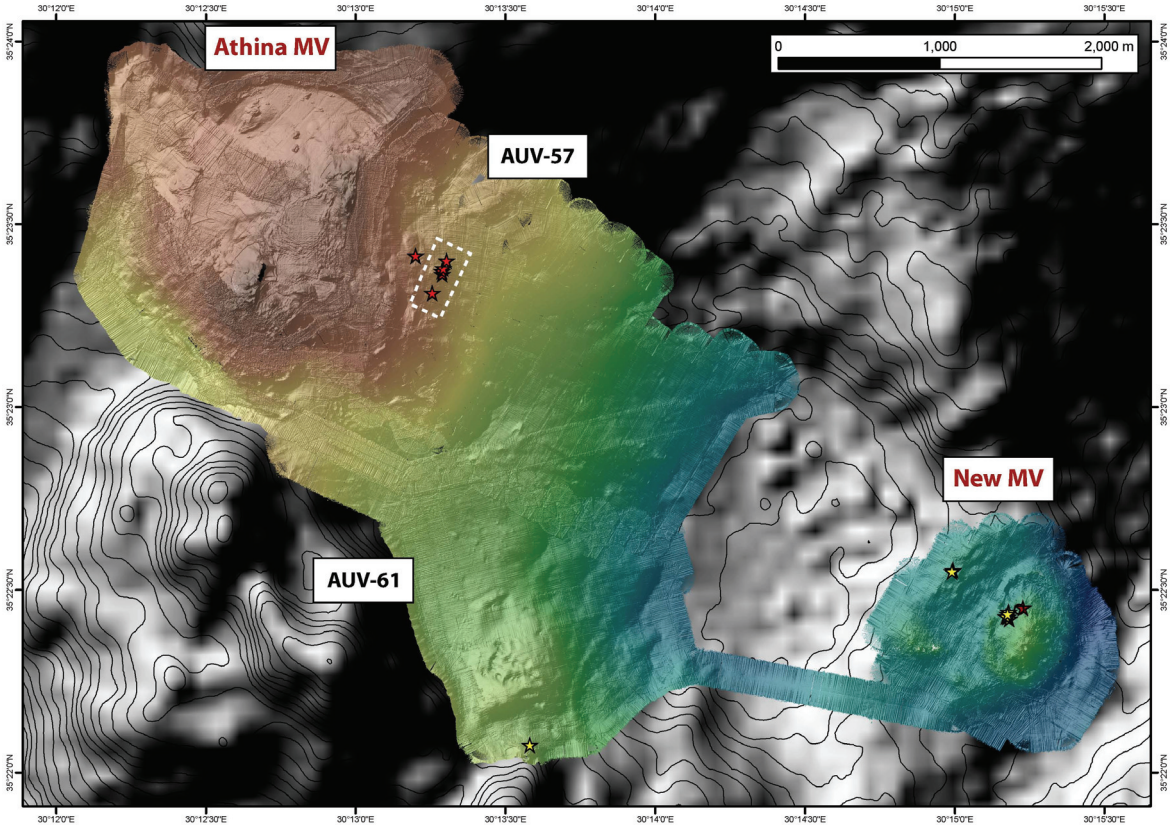

Fig. 25a: Micro bathymetry of Athina Mud Volcano was mapped during three dives from which the last dive (Dive 61) included a small mud volcanic structure not known before the cruise.

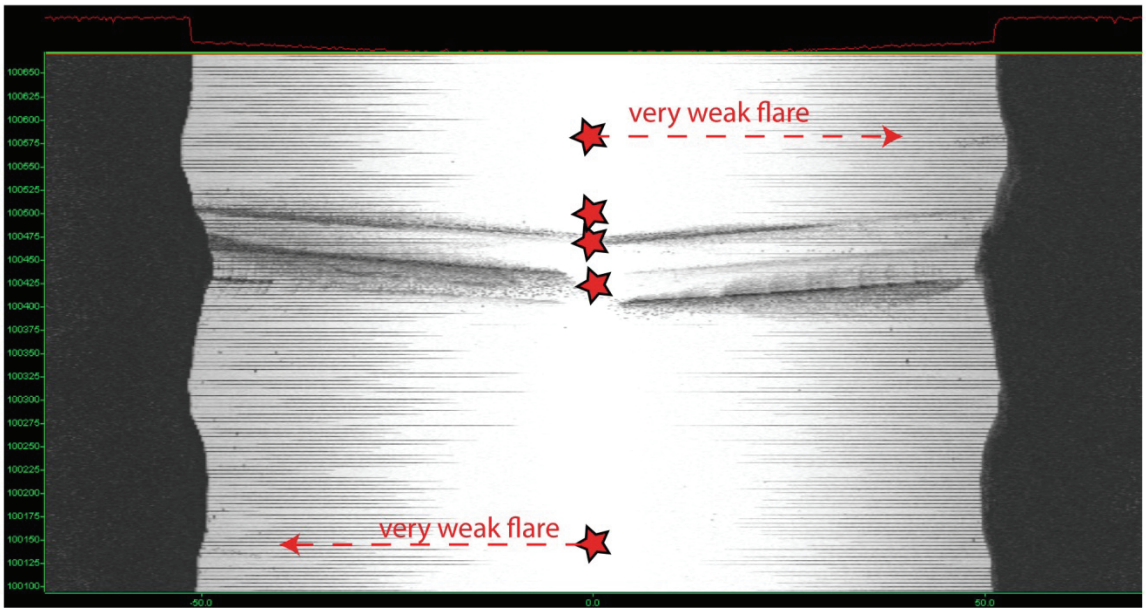

Fig. 25b: Screenshot of the MBES data in PDS2000, illustrating the flare appearance in the sidescan mode and the flare picking (red stars). For location see white box in Fig.25a.

Amsterdam MV: AUV Dives 58, 59, 60

Three dives were conducted at the Amsterdam MV and numerous flares were detected during all three dives. They were either located in the central area or along the surrounding rim of the mud volcano structure (Fig. 26).

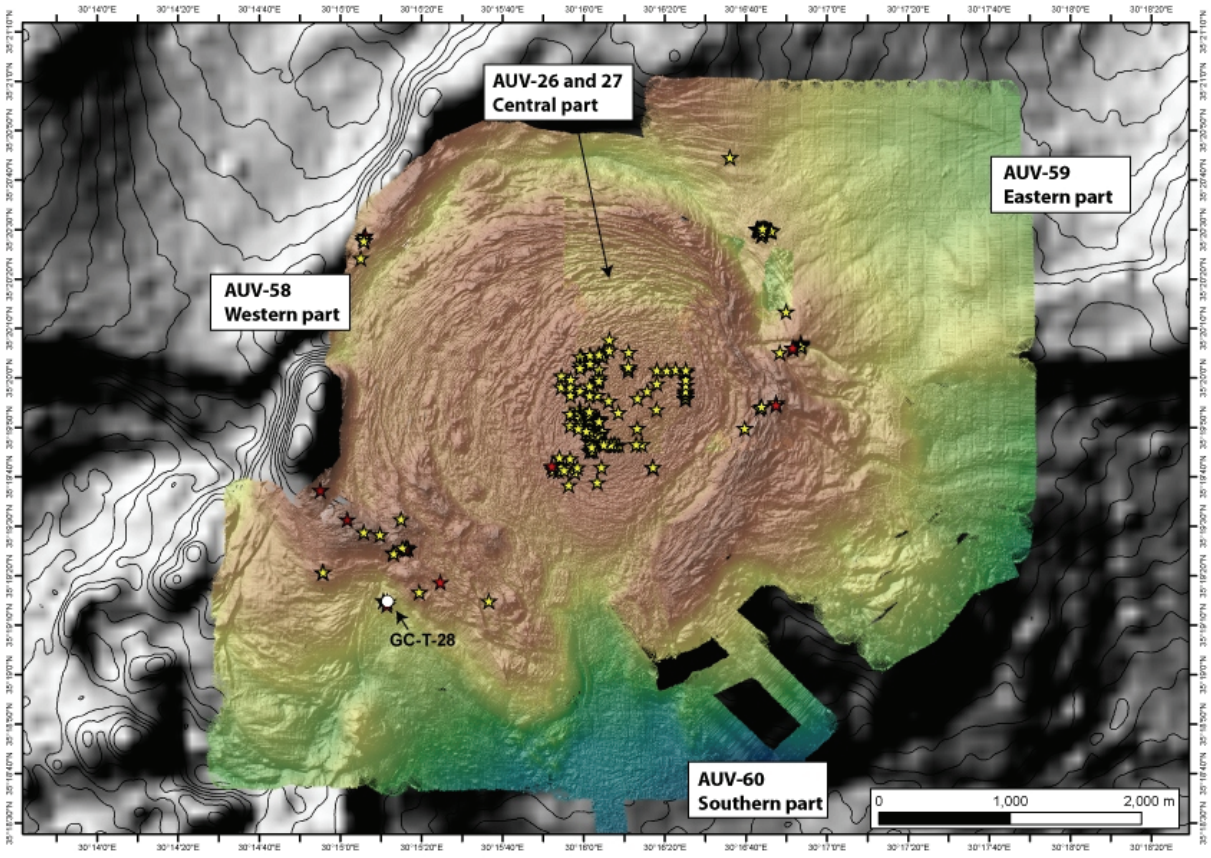

Fig. 26: Compiled map of all AUV maps resulting from dives conducted during an earlier cruise (Dives 26 and 27 during MSM13/4) and Dives 58, 59 and 60 conducted during this cruise. Red stars show flares classified as strong and yellow those with a relatively weak intensity.

5 Station Work with the Autonomous Underwater Vehicle (AUV) MARUM SEAL 5000

(G. Meinecke, J. Renken, U. Spiesecke, T. von Wahl, T. Leymann)

5.1 Introduction

In the year 2006 the MARUM ordered a deep diving autonomous underwater vehicle (AUV), designed as a modular sensor carrier platform for autonomous underwater applications. This AUV was built in Canada by the company International Submarine Engineering (I.S.E.). In June 2007 the AUV "SEAL" was delivered to MARUM and tested afterwards on the French vessel N/O SUROIT (June 2007) and the German R/V POSEIDON (November 2007) in the Mediterranean Sea. Since then, the AUV is in operational mode and was used 8 times on field cruises on-board research vessels (R/V SONNE, R/V METEOR, R/V M.S.MERIAN, R/V POSEIDON, N/O SUROIT) and 2 times in lake studies (Lake Constance, Lake Neuchatel). Therefore, this R/V POSEIDON cruise is the 9th field cruise of MARUM SEAL.

5.2 SEAL Vehicle – Basics

The MARUM AUV Seal is No. 5 of the Explorer-AUV series from the company I.S.E. The AUV is nearly 5.75 m long, with 0.73 m diameter and a weight of 1.35 tons. The AUV consists of a modular atmospheric pressure hull, designed from 2 hull segments and a front and aft dome. Inside the pressure hull, the vehicle control computer (VCC), the payload control computer (PCC), 8 lithium batteries and spare room for additional "dry" payload electronics are located. Actually, the inertial navigation system PHINS and the RESON multibeam-processor are located as dry payload here. The tail and the front section, built on GRP-material, are flooded wet bays. In the tail section the motor, beacons for USBL, RF-radio, Flashlight, IRIDIUM antenna and DGPS antenna are located. In the front section the Seabird SBE 49 CTD, the Sercel MATS 200 acoustic modem, the DVL (300kHz), KONGSBERG Pencil beam (675kHz), the RESON MBES 7125B (400kHz), the PAROSCIENTIFIC pressure-sensor and the BENTHOS dual frequency (100/400kHz) side scan sonar are located. Actually, the SEAL AUV has a capacity of approx. 15 KWh main energy which enables the AUV for approx. 70 km mission-track lengths.

For security aspects, several hard- and software-mechanisms are installed on the AUV to minimize the risk for malfunction, damage and total loss. More basic features are dealing with fault response tables, up to an emergency drop weight, either released by user or completely independent by AUV time-relays itself.

MARUM put special emphasis on open architecture in hard- and software design of the AUV, in order to be as much as possible modular and flexible regarding the vehicle operations. Therefore, the VCC is based to large extend on industrial electronic components and compact-PCI industrial boards and only very rare proprietary hardware boards have been implemented. The software is completely built QNX 4.25 – a licensed UNIX derivate, to large extends open for user modifications. The payload PC is built on comparable hardware components, but running either with Windows and/or Linux.

On the support vessel, the counterpart to the VCC is located on the surface control computer (SCC). It is designed as an Intel based standard PC, also running with same QNX OS and a Graphic User Interface (GUI) to control and command the MARUM SEAL AUV. Direct communication with the

AUV is established via an Ethernet-LAN, either by hard-wired 100mb LAN cable plugged to AUV on deck, or by Ethernet-RF-LAN modem - once vehicle is on water. The typical range of RF-communication is around 1 – 2 km distance to vehicle. Within this range the user has all options to operate the AUV in Pilot-Mode, e.g. to manoeuvre the AUV on water or change vehicle settings. Once the AUV is under water, all communication links were shut down automatically and the AUV has to be in mission-mode, means it is working based on specific user-defined missions.

Despite being in mission-mode it is necessary to communicate with the AUV when it is under water, i.e. asking for actual position, depth and status. To achieve this, on-board the support vessel an acoustic underwater modem with dunking transducer has to be installed (SERCEL MATS modem) communicating with the counterpart on the AUV, on request. Due to limited acoustic bandwidth only rare data sets are available.

5.3 Mission-Mode

The AUV - as dedicated autonomous vehicle - has to be pre-defined operated under water, by demand. As mentioned, only at sea surface manoeuvring by the pilot is possible - once it dives, it will lose communication and therefore must be in a mission-mode. Initialized correctly, fault prevention mechanisms should prevent the AUV for damage/loss in that case.

Simplified, an AUV mission is a set of targets; clearly defined by its longitude, latitude, and a given depth/altitude the vehicle should reach/keep by a given speed of AUV in a distinct time. The AUV needs to be in a definite 3-dimensional underwater space to know exactly its own position over mission time in order to actively navigate on this. To achieve this basic scenario, the AUV is working at sea surface with best position update possible, e.g. DGPS position. Once it dives, it takes the actual position as starting point of navigation, looks for its own heading and the actual speed and calculating its on-going position change based on the last actual position, e.g. method known as dead reckoning. To achieve highest precision in navigation, a combination of Motion Reference Unit (MRU) and Inertial Navigation System (INS) is installed on the MARUM SEAL AUV – the PHINS inertial unit from IXSEA Company. Briefly, the MRU is “feeling” the acceleration of the vehicle in all 3 axis (x,y,z). The INS is built on 3 fibre-optic gyro’s (x,y,z) and gives a very precise/stable heading, pitch and roll information, based on rotation-changes compared to the axis. Even on long duration missions, the position calculated by the AUV will be very accurate based on that technique.

5.4 Mission Planning

In principle and very briefly, it would be accepted by the vehicles VCC to receive a simple list of waypoints as targets for the actual mission (the list has to be in a specific syntax). In order to arrange it more efficient and convenient a graphical planning tool is used for this mission planning. The MIMOSA (© Ifremer) mission planning tool is a software package specially designed to operate underwater vehicles (AUVs, ROVs, glider). The main goal of this software is to plan the current mission, observe to AUV once it is underwater and to visualize gathered data from several data sources and vehicles.

MIMOSA is mainly built on 2 software sources, e.g. an ArcView 9.1 based Graphical Information System (© ESFRI ArcGIS) and professional Navigation Charting Software (© Chersoft UK).

In order to plan a mission the user has to work on geo-referenced charts with a given projection (MERCATOR); either GIS-maps, raster-charts or S-57 commercial electronic navigational charts (ENCs). These basic charts could be enlarged easily with user specified GIS projects, enhanced with already gathered data, e.g. multibeam data, points of interest. Once installed in MIMOSA, one can create AUV missions by drawing the specific mission by mouse or using implemented set of tools (MIMOSA planning mode). Missions created in that way are completely editable, movable to other geographical locations and exportable to other formats. In order to be interpretable by the MARUM SEAL AUV, the created mission will be translated in the I.S.E. specific syntax; a set of targets, waypoints, depth information and timer will be created and written into an export path. From here the mission file can be uploaded via the SCC (support vessel) into the VCC (AUVs control PC); the AUV has its mission and is capable to dive, based on a valid mission plan.

5.5 Mission Observing/Tracking

The MIMOSA planning tool is also used for supervision, e.g. to monitor the vehicle at sea surface and more interesting under water (MIMOSA observation mode). The MIMOSA software is client based, means one dedicated server is used for planning, while the others are in slave/client mode, picking up actual missions. Therefore, position data strings (UDP broadcast data) from the support ship (i.e. R/V POSEIDON / position, heading) are being sent to local network and fed into the MIMOSA software; the same is active for the AUV position data, e.g. DGPS signal once it is on sea surface. During dive the AUV can be tracked automatically via ship-borne ultra short baseline systems (USBL), e.g. IXSEA GAPS or POSIDONIA, using the on-board AUV installed USBL transponder beacon responded signal (delivers position where the vehicle “actually” is).

In addition to this independent position source, vehicles own position (deliver where the vehicle “thinks” it is) can be displayed also. This position is based on transmitted data strings from MATS underwater acoustic modem, only sent from AUV on user request.

To summarize, usually you have displayed in tracking mode:

- position of support vessel (lon/lat and heading)
- either DGPS of AUV during surface track, or
- USBL position (GAPS or POSIDONIA)
- and MATS position (underwater acoustic on request).

5.6 Operational Aspects

In general, MARUM SEAL was used at least 9 times on field cruises so far. Thus, several different vessels have been in operation and on each vessel the handling of the AUV is quite a bit different. In principle, the A-frame seems to be the best position to launch and recovery the AUV, because the tendency to hit ships wall is minimized compared to sideward operation, based on experiences. On R/V POSEIDON 462 the AUV was operated successfully with the main crane at portside of vessel; the gear boom is not appropriate for AUV operations and the A-frame is not tall enough to handle the AUV at stern.

In principle, the AUV can be operated out of the lab, just with simple PC-console racks. On P462 cruise, the AUV operations were run out of a 20” operation/workshop van, located on the main deck

at stern of the vessel. The consoles, file-server and printer are installed in the container, workbench, tools and spares as well.

The SERCEL MATS acoustic transducer was installed into the moon pool of R/V POSEIDON, together with the USBL GAPS positioning antenna.

Prior to launch of AUV, the GAPS as well as the PHINS INS (on-board the AUV) need to be calibrated. Therefore, both systems need to be reset and the support vessel has to be standing still for at least 5 minutes. After that initial phase (INS coarse align), the vessel has to run a rectangular course; square-coarse, 5 minutes at 3-5 knots each line (INS fine align). At the end of that time span and course, the PHINS is in so called “normal mode”, means it has its highest position quality.

5.7 Station Work on RV POSEIDON Cruise P462

During P462 cruise we did 8 dives; 6 dives have been performed without any technical problems, whereas 1 dive was aborted at 50% of mission track due to a broken plane drive and 1 dive was terminated by “low altitude alarm” due to rough terrain. In total, 400.6 km of track lines have been mapped at bottom.

Dive No. 54:
The first dive during P462 was located at Thessaloniki Mud Volcano. The track length at bottom was 63.4 km.

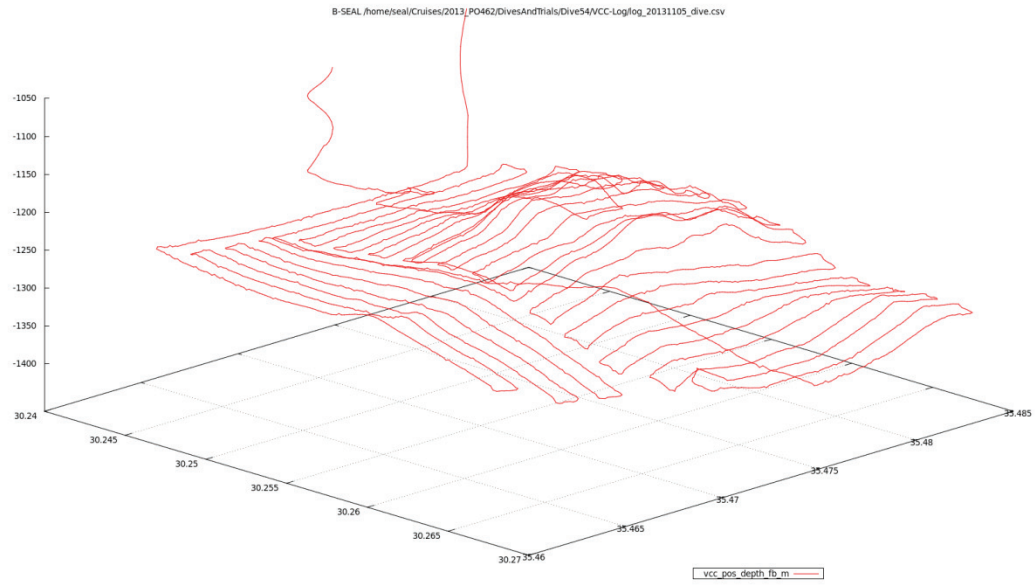

Fig. 27: Dive track of dive no. 54 (Thessaloniki MV), depth of AUV SEAL vs. longitude/latitude.

Dive No. 55:
The second dive during P462 was located at Kazan Mud Volcano. At half of mission duration, the AUV aborted the mission due to broken plane drive, which was broken during a spontaneous bottom avoid task. The track length at bottom was 35.0 km.

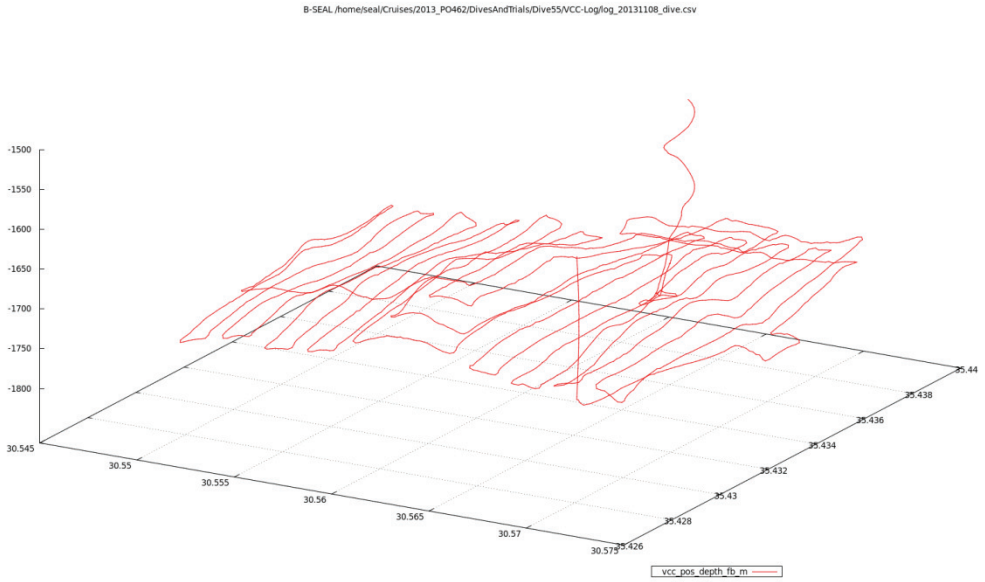

Fig. 28: Dive track of dive no. 55 (Kazan MV), depth of AUV SEAL vs. longitude/latitude.

Dive No. 56:

The third dive during P462 was located at Athina Mud Volcano. The AUV dove down properly, but immediately after start of bottom track the AUV stopped its missions with a “stop level” fault. The track length at bottom was only 1.5 km. The reason for mission abort was a very rough terrain in the landing zone of AUV. Due to a not optimized trim of AUV, the AUV could follow the harsh terrain in “bottom avoid mode” and finally encountered a “low-altitude fault” and stopped its mission.

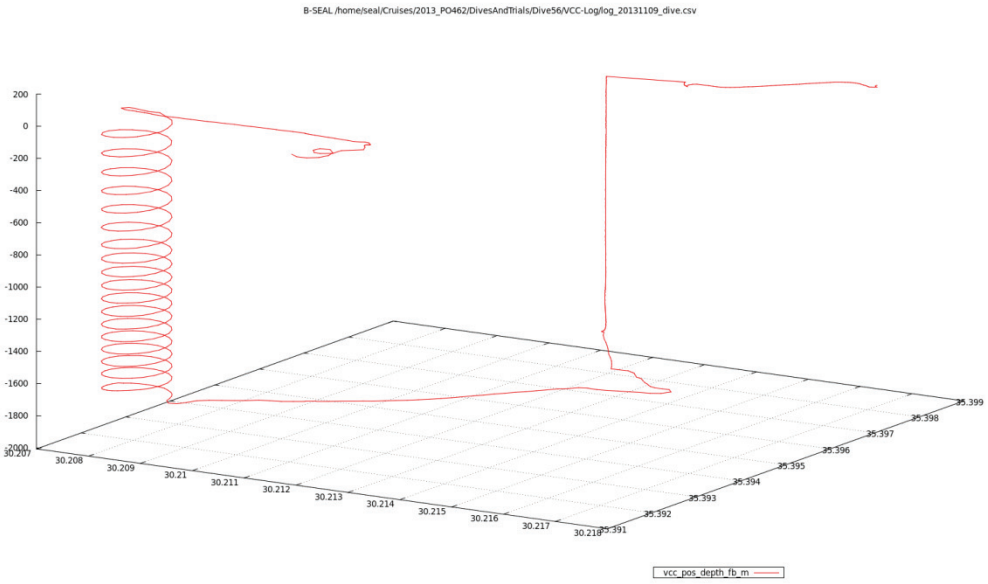

Fig. 29: Dive track of dive no. 56 (Athina MV), depth of AUV SEAL vs. longitude/latitude. Abort due to low altitude alarm.

Dive No. 57:

The fourth dive during P462 was the repeated no. 56 at Athina Mud Volcano. The track length at bottom was 54.5 km.

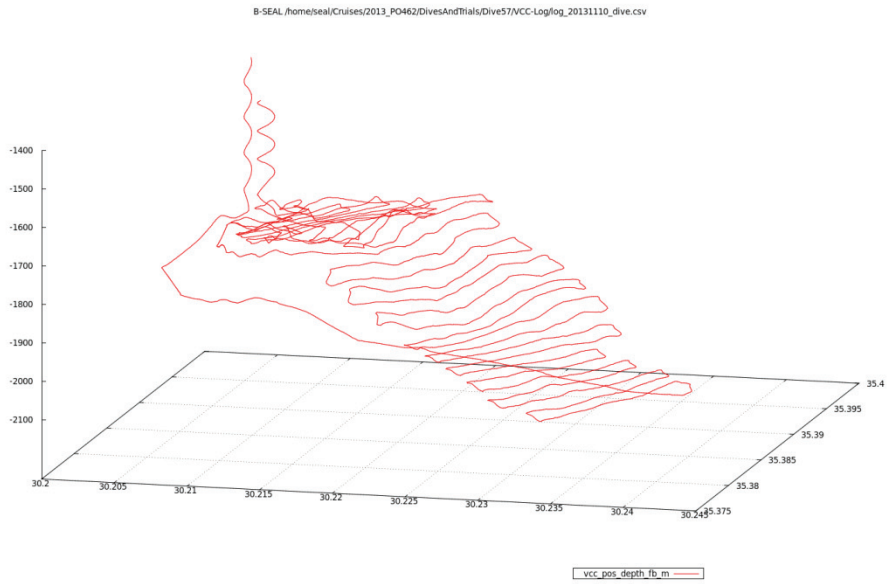

Fig. 30: Dive track of dive no. 57 (Athina MV), depth of AUV SEAL vs. longitude/latitude.

Dive No. 58:

The fifth dive during P462 was no. 58 at Amsterdam Mud Volcano – western part. The track length at bottom was 64.1 km.

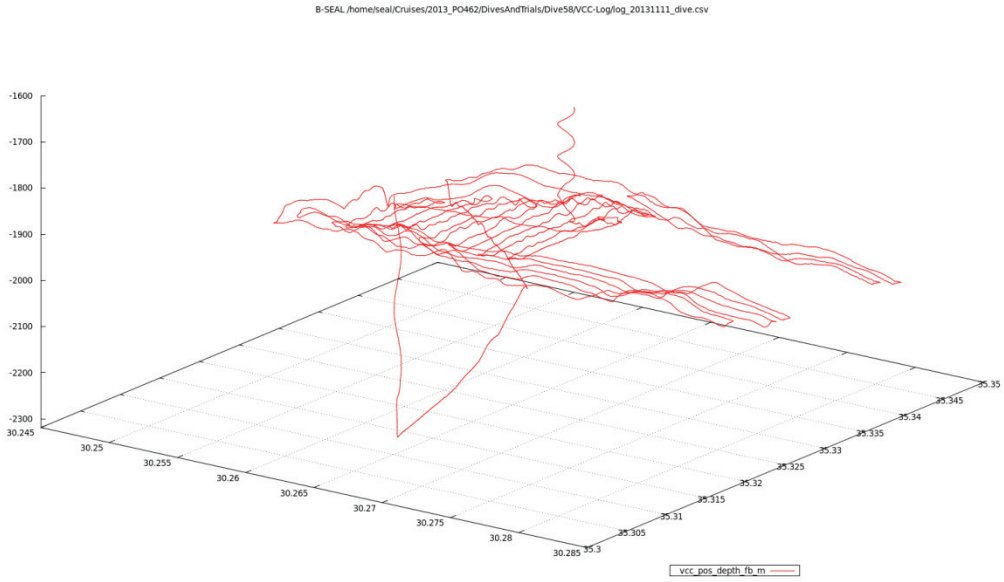

Fig. 31: Dive track of dive no. 58 (Amsterdam MV-west), depth of AUV SEAL vs. longitude/latitude.

Dive No. 59:

The sixth dive during P462 was no. 59 at Amsterdam Mud Volcano – eastern part. The track length at bottom was 65.0 km.

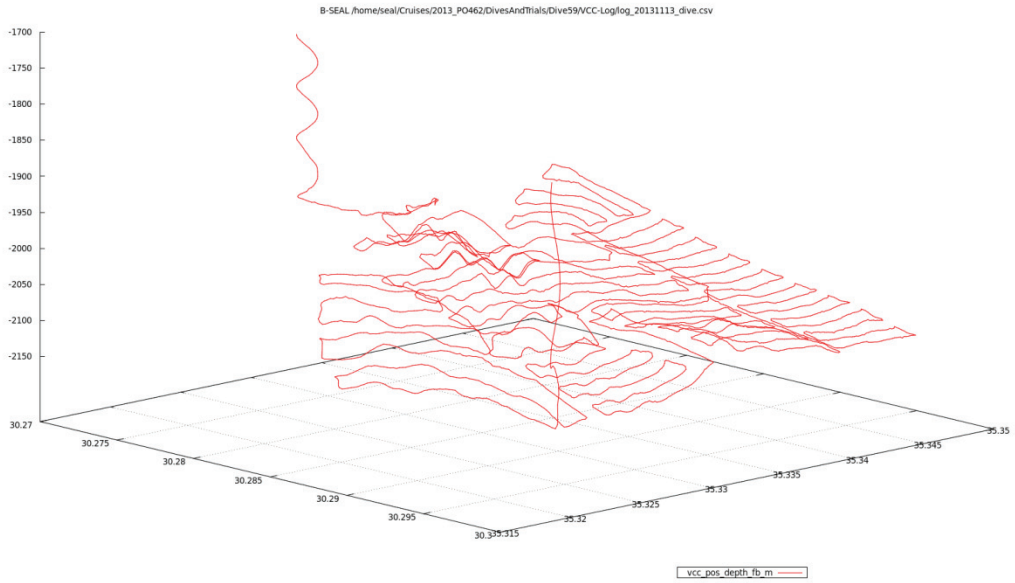

Fig. 32: Dive track of dive no. 59 (Amsterdam MV-east), depth of AUV SEAL vs. longitude/latitude.

Dive No. 60:

The seventh dive during P462 was no. 60 at Amsterdam Mud Volcano – southern part. The track length at bottom was 63.5 km. The mission planning was complex, due to steep slopes and the central valley in between the mission.

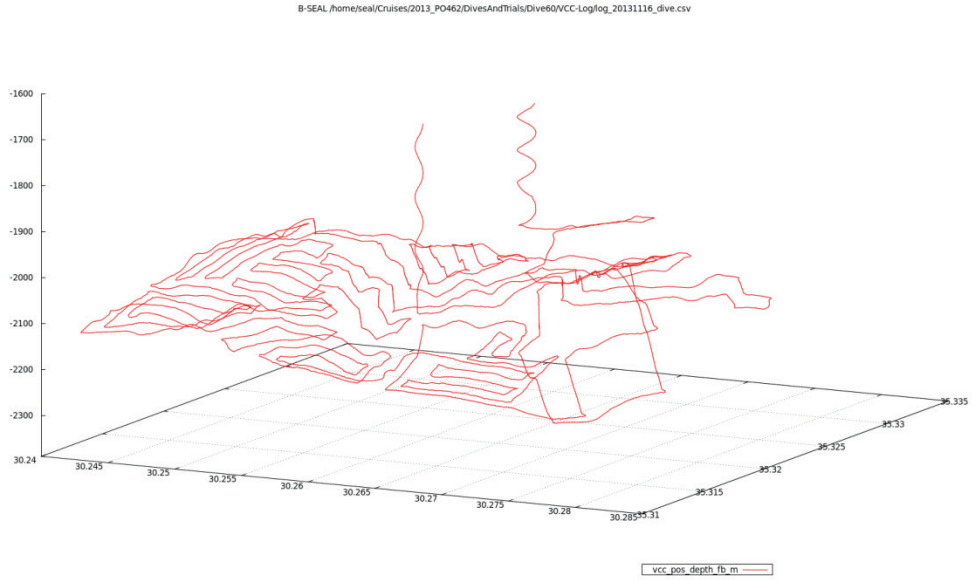

Fig. 33: Dive track of dive no. 60 (Amsterdam MV-south), depth of AUV SEAL vs. longitude/latitude.

Dive No. 61:

The eighth dive during P462 was no. 61 at Athina Mud Volcano, again– southern part. The track length at bottom was 53.6 km. The mission planning was complex, due to rim-mapping and steep slopes at the downhill mission.

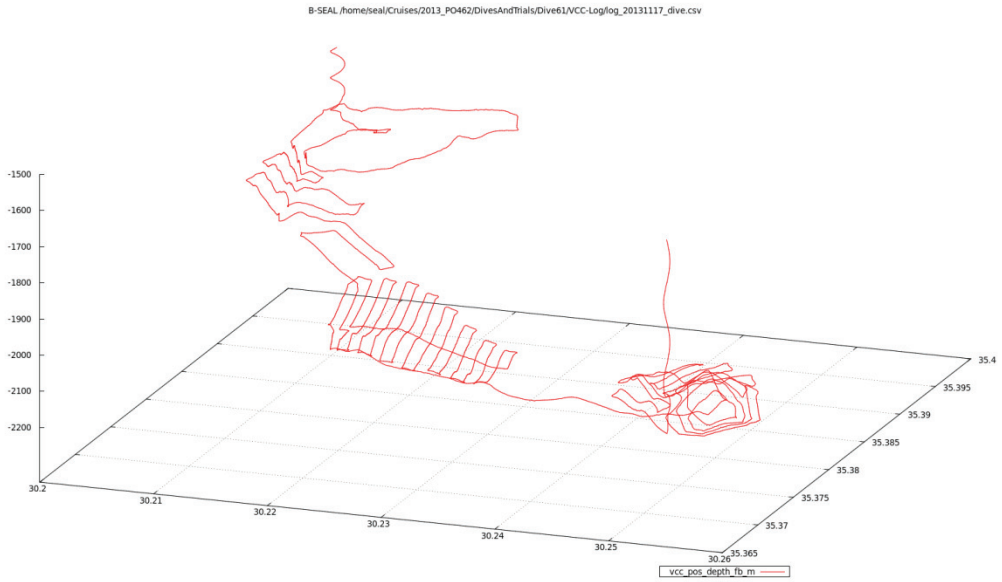

Fig. 34: Dive track of dive no. 61 (Athina MV-south), depth of AUV SEAL vs. longitude/latitude.

6 Sediment Cores

(M. Römer, T. Pape, K. Dehning, G. Bohrmann)

A gravity corer (GC) equipped with a 6 m long cutting barrel and a weight of about 2 tons was used to collect shallow sediment samples. The cutting barrel was either equipped with a flexible plastic foil as a liner which allows for rapid access to gas hydrates or with a PVC-liner for recovery of undisturbed sediments. Onboard RV POSEIDON, the GC was run via winch W3 and the rope velocity during seafloor penetration was adjusted to 1.0, 1.2 or 1.3 m/s, respectively.

At four stations temperature probes were mounted to the cutting barrel and the weight set of the gravity corer for in-situ temperature measurements. At those stations, the gravity corer was left in the sediment for ca. 7 - 10 mins in order to achieve equilibration conditions for sediment temperature. Samples of hydrate-bound gas for analysis in the home lab were prepared from four cores taken at the Thessaloniki MV and two cores from the Kazan MV.

The gravity corer was deployed 28 times during P462 (Table 3) at five different mud volcanoes (Fig. 35).

Table 3: Specifics of gravity corer deployments during P462; gas hydrate samples are listed in the last row.

GC	GeoB #	Area	Plastic foil	PVC-liner	Wire speed (m/s)	T-Sensors	Core recovery (cm)	Hydrate-bound gas
GC-1	17906-1	Thessaloniki MV	X		1.0		500	X
GC-2	17907-1	Thessaloniki MV	X		1.0		15	
GC-3	17907-2	Thessaloniki MV	X		1.3		cc	
GC-4	17908-1	Thessaloniki MV	X		1.2		340	X
GC-5	17909-1	Thessaloniki MV	X		1.2		-	
GC-T-6	17918-1	Athina MV	X		1.0	X	cc	
GC-T-7	17921-1	Thessaloniki MV	X		1.0	X	120	
GC-8	17922-1	Thessaloniki MV	X		1.0		150	
GC-9	17923-1	Thessaloniki MV	X		1.0		65	
GC-10	17924-1	Thessaloniki MV	X		1.2		cc	
GC-11	17925-1	Thessaloniki MV	X		1.0		370	X
GC-12	17926-1	Thessaloniki MV	X		1.0			X
GC-13	17927-1	Thessaloniki MV	X		1.0		190	
GC-14	17930-1	Kazan MV	X		1.0		115	
GC-15	17931-1	Kazan MV	X		1.0		164	
GC-16	17932-1	Kazan MV	X		1.3		230	X
GC-17	17933-1	Kazan MV	X		1.3		304	X
GC-18	17935-1	Athina MV	X		1.3		95	
GC-19	17936-1	New MV	X		1.3		cc	
GC-20	17941-1	Kazan MV	X		1.3		118	
GC-21	17942-1	Kazan MV	X		1.3		87	
GC-22	17943-1	Kazan MV	X		1.3		145	
GC-23	17946-1	Kazan MV	X		1.0		45	
GC-24	17947-1	Kazan MV		X	1.3		228	
GC-25	17950-1	Athina MV	X		1.3		cc	
GC-26	17951-1	Athina MV	X		1.3		370	
GC-27	17952-1	Athina MV	X		1.3		360	
GC-T-28	17964-1	Amsterdam MV	X		1.0	X	54	
GC-T-29	17965-1	New MV	X		1.0	X	225	

cc: material only in core catcher

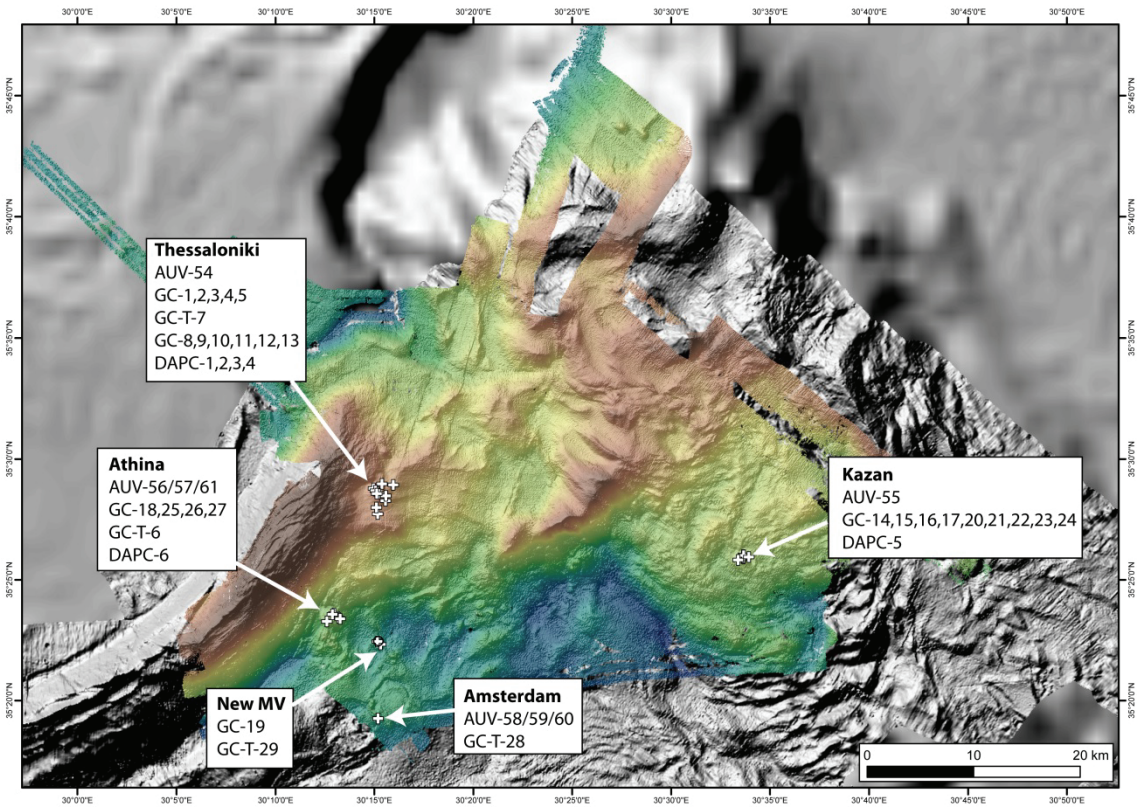

Fig. 35: Overview map of the gravity corer deployments during P462

6.1 Thessaloniki Mud Volcano

At Thessaloniki Mud Volcano several gravity cores haven been taken in order to find a position for shallow gas hydrate sampling using the DAPC. Decisions for the first coring sites have been taken by analyzing multibeam backscatter anomalies and gas emission sites revealed by flare imaging.

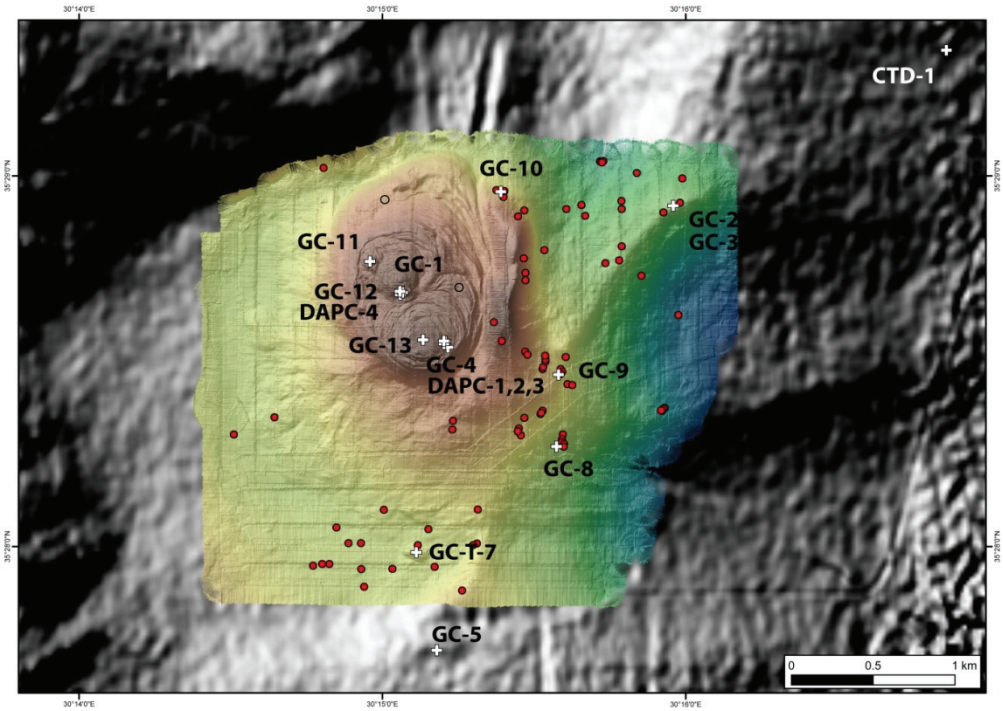

Fig. 36: Gravity corer and DAPC taken at Thessaloniki MV during P462. In color is shown the AUV map as revealed during the cruise (dive 54). Red points illustrate the locations of flares detected during the AUV Dive 54 (preliminary data).

Gravity core GC-1 (Station # 1029-1; GeoB 17906-1) was taken at the center of Thessaloniki MV at 1238 m water depth based on the gas hydrate findings in core AX48-GG1 taken during R/V AEGAEO cruise in October-November 2004 (Perissoratis et al. 2011). The new gravity core from 1238 m water depth covered a sediment sequence of 490 cm mud breccia, composed of a fine-grained clayey matrix enriched by homogenously dispersed rock clasts. The dominantely angular to subangular clasts differ in composition and vary in size. Larger clasts of up to 5 cm in diameter were sampled predominantly below 2 mbsf. Clasts of 2-3 cm in size were found in the upper 2 m of the core. A few gas hydrate pieces were observed between 230-270 and at 380 cmbsf, where a sample for gas analyses was taken. In general the mud appeared moussy which confirmed that gas released from the core during recovery.

Gravity core GC-2 (Station # 1030-1; GeoB 17907-1) and **GC-3** (Station # 1030-2; GeoB 17907-2) were taken approximately 1 nm northeast of the mud volcano at a bathymetric nose which showed a high backscatter signal and an acoustic flare during the survey of the current cruise. A carbonate cemented sediment with densely packed bivalve shells avoided further penetration of the gravity corer and the only 15 cm sediments were recovered below the carbonate with gravity core GC-2 whereas GC-3 contained the carbonate remnants in the core catcher. Clam shells of different sizes are possibly lucinid type bivalves which prove chemosynthetic life and cold seepage on the seafloor.

Fig. 37: Carbonate precipitates and various shells partly from chemosynthetic fauna sampled with GC-3 at an area with high backscatter and gas seepage (left); densely packed shell layer at the surface of gravity core GC-2.

Gravity core GC-4 (Station # 1031-1; GeoB 17908-1) was taken on a morphological peak of the southern plateau of Thessaloniki Mud Volcano in 1258 m water depth. The 340 cm long core is composed of a typical mud breccia with very various clasts occurring throughout. Some clasts of up to 15 cm in diameter were sampled and small gas hydrate specimens were sampled from the core catcher. The upper 80 cm of the core appeared relatively soupy and between 110-115 cmbsf an intensely black sapropel layer was intercalated. Below this sapropel layer a very soupy sediment indicated most probably a past hydrate presence.

Fig. 38: Angular clasts of various origin sampled with GC-4 at the southern top of Thessaloniki Mud Volcano (left); Detail from gravity core GC-7 showing the transition from oxic to sub-oxic/anoxic environment, with several burrow traces and white shells of pteropodes (right).

A coring attempt south but outside of Thessaloniki MV (**gravity core GC-5**; Station # 1032-1; GeoB 17909-1) failed, because the sediment was washed out of the core liner. That position was chosen because we observed a high backscatter signal and a gas flare during a survey before.

Gravity core GC-T-7 (Station # 1044-1**;** GeoB17921-1) was planned based on the preliminary AUV data from Thessaloniki Mud Volcano. A very local elevation of 1-2 m was observed in the micro-bathymetry map combined with a distinct flare in the AUV data. Unfortunately the core was bended and most of the sediments were lost during the complicate recovery procedure of the damaged gravity corer. The penetration of the corer was more than 5 mbsf, however, the recovery was only 120 cm. The uppermost redish brown mud (0-32 cmbsf) with a fine lamination at the bottom is underlain by dray gray mud (32-51 cmbsf) with dense bioturbation traces of various sizes. Below 51 cmbsf the mud changed to light gray mud. Distinct large shells of white pteropodes were found at 32 cm, 106 and 120 cmbsf. Based on the sediment which was attached to the outside core barrel, the deepest deposits, sampled by the corer have been very stiff mud breccia.

Gravity cores GC-8 (Station # 1045-1; GeoB17922-1) at 1302 m water depth and **GC-9** (Station # 1046-1; GeoB17923-1) at 1285 m are both cores from two different positions, where high backscatter and gas flares have been previously observed. The plan was to test those locations for hydrate presence. Both showed a colorful sediment sequence 150 cm and 65 cm long of pelagic deposits without traces of mud breccia. Dark brown mud layers with numerous very fine bioturbation traces and pteropode shells are intercalated with light gray mud and black sapropel layers. GC-9 contained many strongly indurated sediment parts to highly cemented carbonate precipitates. Especially close to the surface light brownish carbonate precipitates with clam shells were present, clearly indicated seafloor seepage.

Gravity core GC-10 (Station # 1047-1; GeoB17924-1) was planned on top of the separated ridge at the eastern side of Thessaloniki Mud Volcano. However, the gravity core could not penetrate into the sediments and therefore no sediment could be sampled.

Gravity cores **GC-11** (Station # 1048-1; GeoB 17925-1), **GC-12** (Station # 1049-1; GeoB 17926-1), **GC-13** (Station # 1050-1; GeoB 17927-1) sampled relatively fresh mud breccia at specific eruption sites on top of the TMV. The locations were chosen based on the AUV micro-bathymetric map. On that map the TMV has two major eruption centers of 400-500 m in diameters and 2 small parasitic eruption centers accompanying the northern outflow. Gravity corer GC-11 and GC-12 sampled those parasitic outflows. GC-11 was 370 cm long and contained small amounts of disseminated gas hydrates from which 2 gas hydrate samples have been taken to measure the gas composition. GC-12 recovered a mud breccia which contained dispersed gas hydrates in the uppermost part of the core. The record of core GC-13 was 190 cm revealed mud breccia with moussy fabric throughout, however, gas hydrate specimen could not more be observed.

6.2 Athina Mud Volcano

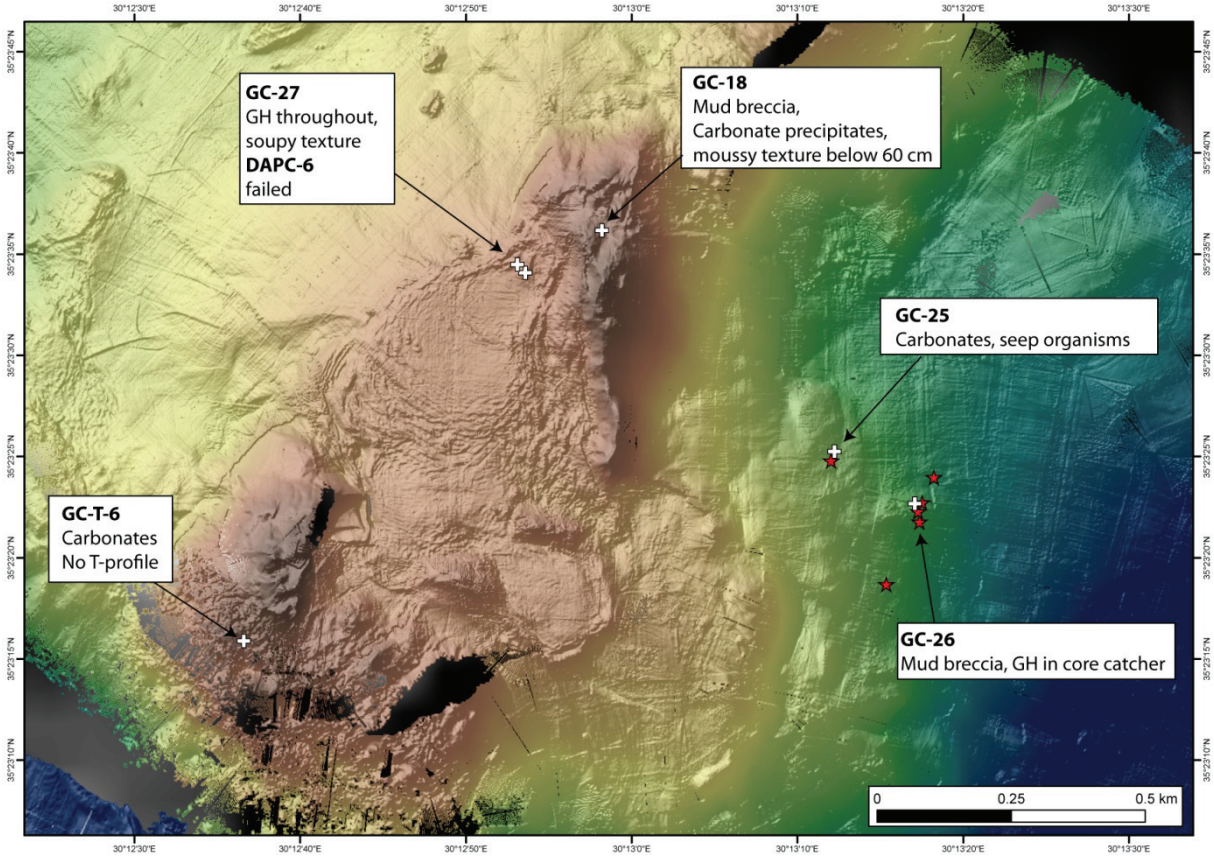

Fig. 39: Positions of the five gravity cores and a DAPC deployment during P462 at Athina MV.

Gravity core GCT-6 (Station # 1041-1; GeoB17918-1) was taken on Athina Mud Volcano on the southern peak in 1793 m water depth. The area was explored by ROV QUEST Dive 135 during M70 in 2006 and it was found that there is active seepage on the seafloor (Bohrmann et al. 2008). The gravity corer equipped with MTLs could not penetrate, because of the highly cemented seafloor and only carbonate fragments were sampled. The precipitates of light yellow color are highly porous and showed several angular clasts cemented by carbonate. Clam shells and worm tubes were also associated.

Fig. 40: Precipitates of pure seepage-related carbonate and various shells partly sampled from core-top in gravity core GC-T-6 of AthMV in an area with high backscatter and gas seepage (left); examples of clasts sampled in the mud breccia with GC-11 at the northern top of Thessaloniki Mud Volcano (right).

Gravity core GC-18 (Station # 1058-1; GeoB17935-1) sampled the northeastern summit of the volcano, whereas the previous gravity corer GCT-6 sampled the southern peak. Since the AUV micro-bathymetry map was not available it was not clear where recent eruptions of the volcano occured. During GC-18 the corer sampled 95 cm of sediments with a mud breccia at the base. The uppermost 15 cm revealed the oxic conditions close to the seafloor where many dead clam shells are present. Between 50-60 cmbsf the deposits appeared indurated by carbonate precipitation. No gas hydrates have been observed in the core.

On Athina Mud Volcano three further gravity cores were selected to deploy at specific targets. Gravity core GC-25 (Station # 1073-1; GeoB17950-1) sampled seep carbonate fragments and chemosynthetic animals on a well pronounced gas flare on the flank of Athina Mud Volcano. Gravity core **GC-26** (Station # 1074-1; GeoB17951-1) sampled a second gas flare location nearby and retrieved below 50 cmbsf a clear sequence of 320 cm sediments which showed 4 different mud flow units, whereby the units are clearly to distinguish based on color and content of mud clasts. A last gravity corer taken during that day in the centre of the obvious mud eruption retrieved 360 cm of fluidized and moussy mud breccia. The high water content was clearly released from decomposing gas hydrates from which we could only observe very tiny crystals.

6.3 Kazan Mud Volcano

First, three sites have been sampled on Kazan Mud Volcano with four gravity cores. Kazan Mud Volcano forms an isolated oval-shaped hill in north-south direction well defined by the 1700 m bathymetric contour. Gravity core **GC-14** (Station # 1053-1; GeoB17930-1) at the northern end of the elevation recovered 115 cm gray mud breccia with angular clasts up to 2 cm in diameter. No hydrates have been found. Gravity cores **GC-15** (Station # 1054-1; GeoB17931-1) and **GC-16** (Station # 1055-1;

GeoB17932-1) have been both taken in the center of the volcanic elevation approximately at the same position. Both cores had a brown oxic layer of 5-8 cm thickness on top and below the typical gray mud breccia with various clasts of different composition. Whereas GC-15 recovered 160 cm sediments, recovery of GC-16 was 230 m. Gas hydrate was distributed and occurred in very tiny crystals and only a very few hydrate pieces could be sampled. The sampling procedure took a while and the cores stayed in the warm upper water mass of the ocean quite a while before the gas-hydrated sediments came on deck for further sampling. A gravity core **GC-17** (Station # 1056-1; GeoB17933-1) was scheduled just a few tens of meters to the north of KMV and recovered a sequence of 304 cm mud breccia with lots of smaller and larger clasts. Gas hydrate crystals occurred below 2 mbsf throughout as dispersed small specimen.

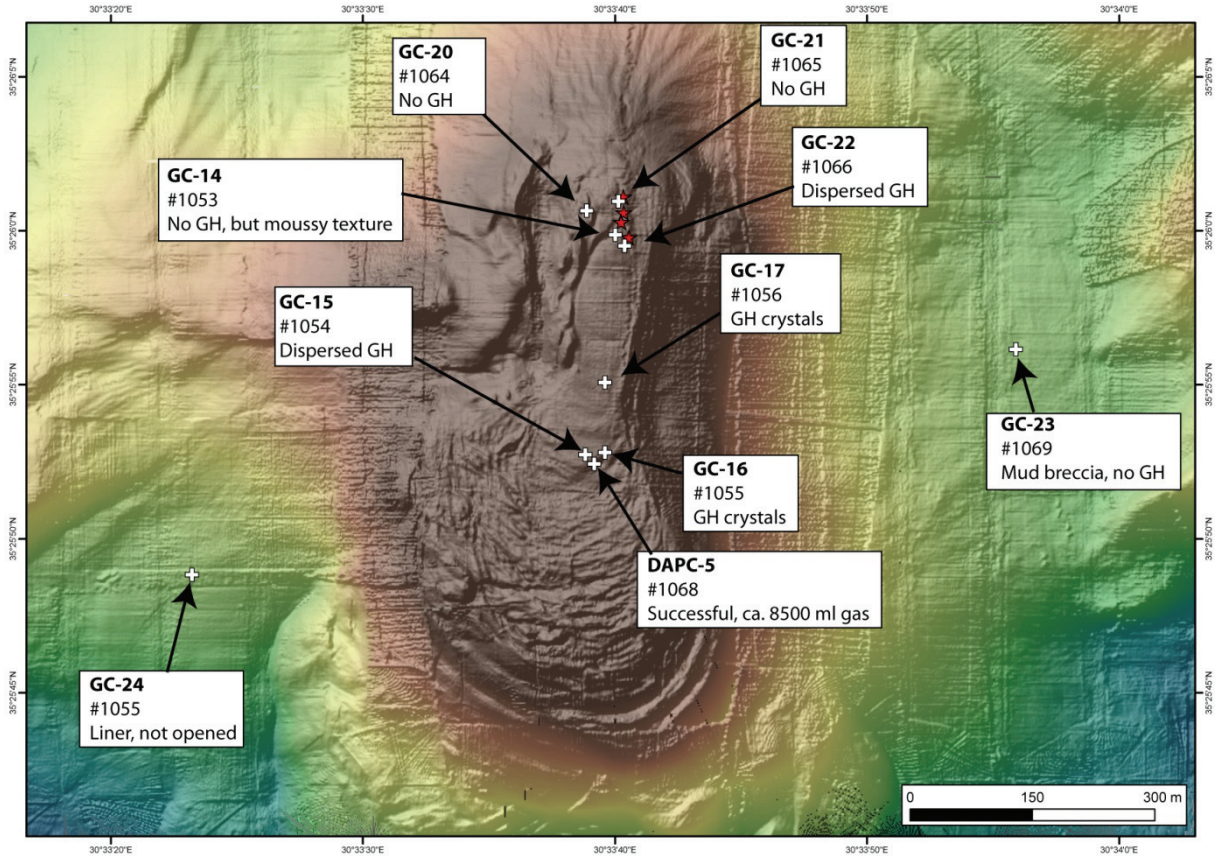

Fig. 41: Positions of gravity cores and DAPC deployments at Kazan MV taken during P462.

The AUV micro-bathymetry map from Kazan Mud Volcano indicated relatively recent eruptions at the northern top and therefore we took three more gravity cores in that area, during which we tried to sample specific elevations on the seafloor. From these three cores **GC-20** (Station # 1064-1; GeoB17941-1), **GC-21** (Station # 1065-1; GeoB17942-1), and **GC-22** (Station # 1066-1; GeoB17943-1) only GC-22 contained very small crystals of gas hydrates, whereas the other two cores only revealed gas expansion structures like moussy fabric. All three cores sampled mud or very stiff clay breccia, especially the latter two. Beside other mud clasts very light, partly fragile clasts have been obvious in the cores. Further sampling on Kazan Mud Volcano was performed east of the center where a high backscatter signal and gas emissions have been recorded in the AUV multibeam data. Gravity core **GC-23** (Station # 1069-1; GeoB 17946-1) sampled 45 cm mud breccia from which the uppermost 4 cm was brownish and the 41 cm below gray containing many white clasts which seem to be unique for Kazan Mud Volcano. Gravity corer **GC-24** (Station # 1070-1; GeoB 17947-1) sampled the mud breccia

west of the center and was taken within a liner to study the approximately age of mud breccia in the home lab.

6.4 New Mud Volcano

On the way to Amsterdam Mud Volcano a gravity corer was deployed southeast of Athina MV on a small elevation which showed a distinct high backscatter signal. Unfortunately the gravity corer **GC-19** (Station # 1059-1; GeoB17936-1) could not penetrate into the sediments. There was no recovery except some carbonates and clam shells in the core catcher.

Fig. 42: Carbonate crust with densely packed small bivalve shells from core top of gravity core GC-19 (left); Samples include a tubeworm, bivalve shells, gastropods and spines of sea urchins (right).

After the successful AUV Dive 61 mapping the New Mud Volcano (Fig. 43), a second gravity core was taken NW of the top, where three flares indicated active degassing. Gravity core **GC-T-29** (Station # 1087-1; GeoB17965-1) nevertheless revealed no signs of gas-rich sediments or gas hydrate occurrence. The core recovered 225 cm sediments with few bivalve shells and lots of pteropods but lacking clasts or carbonates. The lower three MTLs were in the sediments but did not record elevated temperatures.

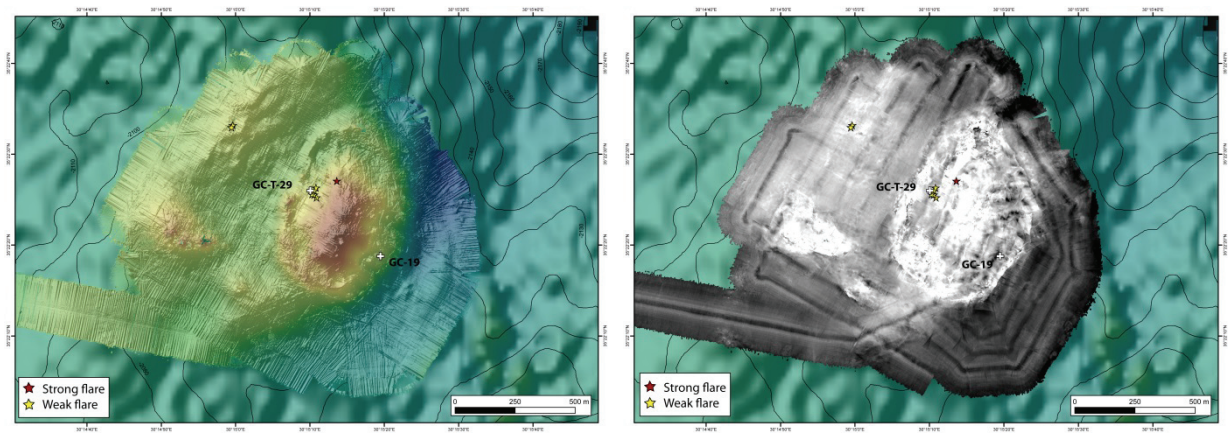

Fig. 43: New MV high-resolution bathymetric map revealed from AUV dive 61 (left) with core positions and flare locations. Backscatter map retrieved from the data of AUV Dive 61 indicating the high backscatter signature of the New MV (right).

6.5 Amsterdam Mud Volcano

After mapping the Amsterdam MV with the AUV, a small circular and mounded structure in its southwestern part became visible. In addition, three flares cluster close together at its center and **GC-T-28** (Station # 1086-1; GeoB17964-1) was aimed to be deployed at the top (Fig. 44). The core recovery revealed 54 cm mud breccia from which the upper 5 cm was brownish with numerous shells. Unfortunately, no signs for gas or gas hydrates were visible and no elevated temperatures were measured with the MTLs equipped on the gravity core.

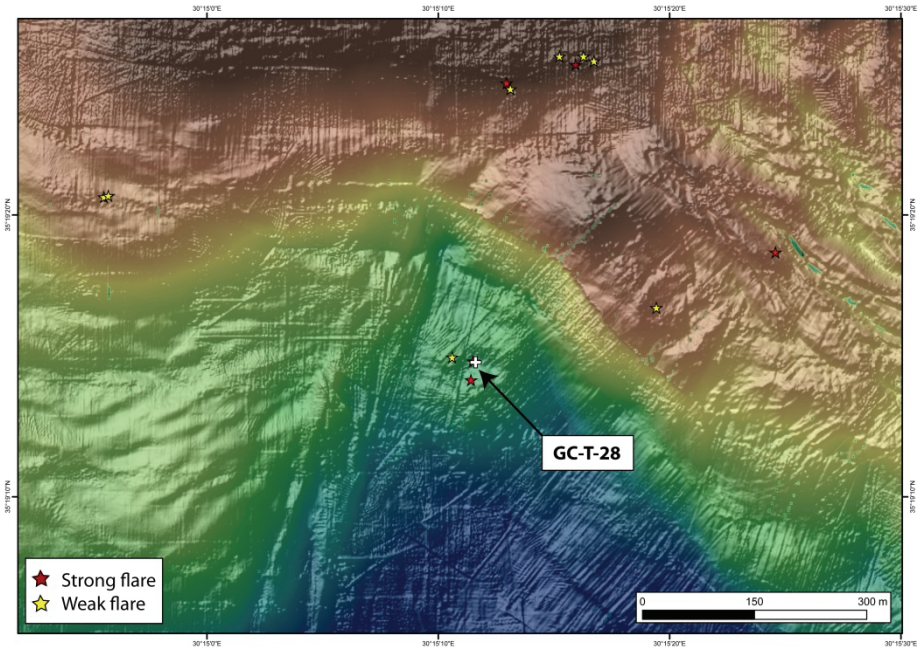

Fig. 44: High-resolution bathymetric map achieved from AUV Dive 60 showing the area southwest of the Amsterdam MV. A mounded structure is visible, where three flares are located at the top and GC-T-28 was deployed.

7 Dynamic Autoclave Piston Corer

(T. Pape, K. Dehning)

The Dynamic Autoclave Piston Corer (DAPC) allows collecting and preserving cores of shallow sediment under in-situ hydrostatic pressure (Abegg et al., 2008). This tool enables to preserve gas hydrates contained in the cores within their stability field during core recovery. Subsequent determinations of gas and gas hydrate volumes contained in the core can be performed by controlled degassing paralleled by gas volume determinations.

The DAPC principally consists of a ca. 2.65 m long core cutting barrel housing a PVC core liner at the initial stage of deployment and a pressure chamber. For coring, contact of a trigger weight mounted to a release mechanism with the seafloor induces release of the system which penetrates the seafloor in a free-fall mode. By heaving of the DAPC subsequent to seafloor penetration, the core liner is drawn through a ball valve into a pressure chamber at its lower end. Finally the pressure chamber is closed gas tight by rotation of the ball valve and by movement of the piston into its bearing on top. During P462 the DAPC was run via winch W3 and deployed at six stations.

DAPC-1 (GeoB 17910-1)

The first DAPC station during P462 was performed at the same position as GC-4 (SE top of Thessaloniki MV, 35°28.538N, 30°15,217E at 1243.5 mbsl), which recovered gas hydrate specimen in a mud breccia matrix and additionally revealed indications for in-situ presence of hydrates below a sapropel layer. The 236 cm long core retrieved with the DAPC contained light grey mud breccia with a slightly moussy texture and a high density of cm-sized clasts throughout the core. A void between 48 and 73 cmbsf pointed at gas expansion during recovery. Core DAPC-1 did not reveal in-situ pressure inside the pressure chamber as the lower part of the liner was stuck in the ball valve and was not completely drawn into the pressure chamber. Therefore, neither the ball valve nor the piston could be moved into their final positions during recovery.

DAPC-2 (GeoB 17913-1)

The second DAPC station was a repetitive station conducted at the same position as GC-4 and DAPC-1 (DAPC-2: 35°28.547N, 30°15.204E at 1248.0 mbsl). Accordingly the core collected slightly moussy mud breccia with several cm-sized clasts and a few clasts > 5cm in size. The total core length was 248.5 cm. Most probably due to the same mechanical problems, which apparently could not be resolved after station DAPC-1 core, core DAPC-2 also revealed no in situ pressure inside the pressure chamber.

DAPC-3 (GeoB 17916-1)

Core DAPC-3 was again a repetitive station of DAPC-1 and -2 (DAPC-3: 35°28.555N, 30°15.204E at 1241.0 mbsl). The core collected was 43 cm in length and contained mud breccia with a slightly moussy texture and several clasts embedded. Due to gas leakage, which was believed to be caused by imperfect positioning of the ball valve in its final bearing, core DAPC-3 did not reveal any gas pressure.

DAPC-4 (GeoB 17929-1)

The fourth DAPC station was performed at NW Thessaloniki MV of DAPC stations 1 – 3 (DAPC-4: 35°28.689N, 30°15.059E at 1245.3 mbsl). The core did not reveal gas pressure inside the pressure

chamber, since the lower (second) O-ring positioned inside the top of the pressure chamber was damaged during heaving and hampered movement of the piston into its final position. During extraction of the core liner abundant sediment and small clasts were observed within the space between liner and pressure chamber. The core was 46 cm in total length and contained mud breccia with mm- to cm-sized clasts in high density.

DAPC-5 (GeoB 17945-1)

Station DAPC-5 was carried out at the Kazan MV (35°25.874N, 30°33,653E at 1668.0 mbsl) at the same position as GC-16 that contained tiny gas hydrates embedded in a mud breccia matrix. Station DAPC-5 was the first completely successful deployment of the DAPC during cruise P462. The recovery pressure was approx. 190 bar and the total gas volume of gas released during controlled degassing was 8500 ml. The respective volumetric gas-sediment ratio of the ca. 65 cm long core, that entirely contained grey mud breccia, was approx. 2.4. Gas samples were taken for analysis of molecular and isotopic compositions in the home lab.

DAPC-6 (GeoB 17952-2)

Core DAPC-6 was taken at an active center in the northern part of the Athina MV (35°23.569N, 30°12,909E at 1772.3 mbsl) at the same position as core GC-26 which upon recovery showed several layers of very moussy mud breccia, the presence of tiny gas hydrates, and intense gas bubbling nearly throughout the entire core.

Station DAPC-6 failed. While the cutting barrel completely penetrated into the seafloor, the release mechanism was not activated and, consequently, the piston was not drawn from its initial position at the lower end of the liner. The inactivity of the release mechanism was attributed to insufficient resistivity of the seabed against the impact of the trigger weight.

8 In-situ Sediment Temperature Measurements

(T. Feseker, M. Roemer)

8.1 Objectives

The ascent of warm fluids and mud at mud volcanoes creates temperature anomalies at the seafloor. Quantification of these anomalies yields information about the mode of emission and seepage rates. In general, the geothermal gradient at the seabed is a good indicator of mud volcano activity. In addition, the temperature distribution in the sediment determines the extent of the gas hydrate stability zone. In situ sediment temperature measurements thus provide information about the activity of mud volcanoes and the potential for gas hydrate formation.

8.2 Methods

In-situ sediment temperature measurements were performed using miniaturized temperature loggers (MTLs) mounted on outriggers attached to the barrel of a gravity corer. In four cases, a regular coring barrel was used in order to obtain a sediment core at the same time. In addition, 16 measurements were performed using a corer barrel with a closed tip. This way, the instrument could be used for multiple penetrations in a row without bringing the instrument back on deck. At all stations, the positioning of the instrument was controlled using a GAPS USBL transponder attached to the wire 50 m above the instrument.

The MTLs were programmed to continuously record temperature readings at an interval of one second. The relative resolution of the MTL measurements is around 0.6 mK. Intercalibration of the loggers in the water column before penetration resulted in a precision of around 2 mK. Equilibrium sediment temperatures will be calculated by extrapolation from the recorded temperature time series. Absolute depth of the profiles is estimated from the equilibrium temperatures in relation to the bottom water temperature.

8.3 Preliminary Results

In-situ temperature measurements in combination with regular gravity coring were attempted at four sites on Athina MV, Thessaloniki MV, Amsterdam MV, and at a newly discovered mud volcano (Tab. 4). At Athina MV, penetration failed due to thick carbonate crusts at the seabed, as evidenced by pieces of the crust found in the core catcher. At the three other mud volcanoes, only slightly elevated sediment temperatures pointed to low levels of activity.

Multi-penetration measurements using the closed corer barrel were performed along transect lines across Athina MV and Kazan MV (Tab. 5). At Athina MV, these measurements revealed moderate activity close to the northern tip of the mud volcano with temperatures of up to more than 15 °C at 5 to 10 m below the seabed. At the warmest locations, the measurements were disturbed due to movements of the corer, most probably due to the low stability of the sediment. Away from this apparent center, the temperature gradients were decreasing rapidly. At Kazan MV, the absence of significant sediment temperature anomalies suggested that this mud volcano is inactive at present.

Table 4: In-situ sediment temperature measurements in combination with gravity coring

Station	GeoB #	Date	Start	End	Target MV	Lat N	Lon E	
1041-1	17918-1	11/6/13	11:11	11:20	Athina	35° 23.265'	30° 12.610'	failed
1044-1	17921-1	11/7/13	04:34	04:44	Thessaloniki	35° 27.984'	30° 15.112'	
1086-1	17964-1	11/18/13	10:47	10:55	Amsterdam	35° 19.246'	30° 15.194'	
1087-1	17965-1	11/18/13	12:23	12:30	New MV	35° 22.433'	30° 15.168'	

Table 5: Multi-penetration in situ sediment temperature measurements with a closed corer barrel

Station	GeoB #	Date	Start	End	Target MV	Lat N	Lon E	
1080-2	17958-1	11/16/13	08:21	08:29	Athina	35° 23.576'	30° 12.887'	
1080-2	17958-2	11/16/13	08:51	08:59	Athina	35° 23.549'	30° 12.859'	
1080-2	17958-3	11/16/13	09:26	09:34	Athina	35° 23.495'	30° 12.820'	
1080-2	17958-4	11/16/13	10:08	10:17	Athina	35° 23.379'	30° 12.779'	
1080-2	17958-5	11/16/13	10:43	10:53	Athina	35° 23.312'	30° 12.913'	
1085-1	17963-1	11/18/13	06:39	06:48	Athina	35° 23.564'	30° 12.871'	
1085-1	17963-2	11/18/13	07:09	07:16	Athina	35° 23.610'	30° 12.950'	
1085-1	17963-3	11/18/13	07:59	08:00	Athina	35° 23.416'	30° 13.205'	failed
1085-1	17963-4	11/18/13	08:25	08:36	Athina	35° 23.370'	30° 13.278'	
1089-1	17967-1	11/19/13	06:51	06:59	Kazan	35° 25.923'	30° 33.935'	
1089-1	17967-2	11/19/13	07:30	07:39	Kazan	35° 25.832'	30° 33.652'	
1089-1	17967-3	11/19/13	07:55	08:02	Kazan	35° 25.872'	30° 33.651'	
1089-1	17967-4	11/19/13	08:16	08:24	Kazan	35° 25.917'	30° 33.658'	
1089-1	17967-5	11/19/13	08:35	08:42	Kazan	35° 25.958'	30° 33.666'	
1089-1	17967-6	11/19/13	09:00	09:07	Kazan	35° 26.000'	30° 33.654'	
1089-1	17967-7	11/19/13	09:20	09:27	Kazan	35° 26.024'	30° 33.659'	

9 References

Abegg F, Hohnberg HJ, Pape T, Bohrmann G and Freitag J (2008). Development and application of pressure-core-sampling systems for the investigation of gas- and gas-hydrate-bearing sediments. Deep Sea Research Part I: Oceanographic Research Papers 55(11): 1590-1599.

Aloisi G, Pierre C, Rouchy JM, Foucher JP and Woodside JM (2000) Methane-related authigenic carbonates of eastern Mediterranean Sea mud volcanoes and their possible relation to gas hydrate destabilisation. Earth and Planetary Science Letters 184(1): 321-338.

Bohrmann G and cruise participants (2008) Report and preliminary results of R/V METEOR Cruise M70/3, Iraklion - Iraklion, 21 November - 8 December, 2006. Cold Seeps of the Anaximander Mountains/Eastern Mediterranean. Berichte aus dem Fachbereich Geowissenschaften der Universität Bremen, 262, 75 pages. Department of Geosciences, Bremen University.

Caress DW, Chayes DN (2001) Improved Management of Large Swath Mapping Datasets in MB-System Version 5, Abstract OS11B-0373. Eos Trans. Fall Meet. Suppl., 82(47).

Charlou JL, Donval JP, Zitter T, Roy N, Jean-Baptiste P, Foucher JP, Woodside JM (2003) Evidence of methane venting and geochemistry of brines on mud volcanoes of the eastern Mediterranean Sea. Deep Sea Research Part I: Oceanographic Research Papers 50: 941-958.

Chaumillon A, Cita MB, Della Vedova B, Fusi N, Mirable L, Pellis G, (1995) Geophysical evidence of mud diapirisim on the Mediterranean ridge accretionary complex. Marine Geolophys.Res.17: 15-141.

DeMets C, Gordon RG, Argus DF, Stein S (1994) Effect of recent revisions to the geomagnetic reversal time scale on estimates of current plate motions. Geophys. Res. Lett. 21: 2191-2194.

Dewey JF, Sengor CAM, (1970) Aegean and surrounding regions: complex multiple and continuum tectonics in a convergent zone. Geo.Soc.Am.Bulletin 90: 84-92.

Huguen RR, Hensen C, Lange G (2005) Pore water geochemistry of eastern Mediterranean mud volcanoes: Implications for fluid transport and fluid origin. Marine Geology 225: 191-208.

Limonov AF, Woodside JM, Cita MB and Ivanov MK (1996) The Mediterranean Ridge and related mud diapirism: a background. Marine Geology, 132(1-4): 7-19.

Lykousis V, Alexandri S, Woodside J, de Lange G, Dählmann A, Perissoratis C, Heeschen K, Ioakim C, Sakellariou D, Nomikou P, Rousakis G, Casas D, Ballas D, Ercilla G (2009) Mud volcanoes and gas hydrates in the Anaximander mountains (Eastern Mediterranean Sea). Marine and Petroleum Geology 26(6): 854-872.

Lykousis V, Alexandri S, Woodside J, Nomikou P, Perissoratis C, Sakellariou D, De Lange G, Dahlmann A, Casas D, Rousakis G, Ballas D, Ioakim C (2004) New evidence of extensive active mud volcanism in the Anaximander mountains (Eastern Mediterranean): The "ATHINA" mud volcano." Environmental Geology 46: 1030-1037.

McClusky S, Bassalanian S, Barka A, Demir C, Ergintav S, Georgiev I, Gurkan O, Hamburger M, Hurst K, Hans-Gert HG, Karstens K, Kekelidze G, King R, Kotzev V, Lenk O, Mahmoud S, Mishin A, Nadariya M, Ouzounis A, Paradissis D, Peter Y, Prilepin M, Relinger R, Sanli I, Seeger H, Tealeb A, Toksaz MN, Veis G (2000) Global Positioning system constraints on plate kinematics and dynamics in the eastern Mediterranean and Caucasus. Journal of Geophysical Research, 105 (B3): 5695-5719.

Pape T, Kasten S, Zabel M, Bahr A, Abegg F, Hohnberg HJ, Bohrmann G (2010) Gas hydrates in shallow deposits of the Amsterdam mud volcano, Anaximander Mountains, Northeastern Mediterranean Sea, Geo-Marine Letters 30: 187-206.

Perissoratis C, Ioakim C, Alexandri S, Woodside J, Nomikou P, Dählmann A, Casas D, Heeschen K, Amman H, Rousakis G, Lykousis V (2011) Thessaloniki Mud Volcano, the Shallowest Gas Hydrate-

Bearing Mud Volcano in the Anaximander Mountains, Eastern Mediterranean, Journal of Geological Research, 11 pages.

ten Veen JH, Woodside JM, Zitter TAC, Dumont JF, Mascle J, Volkonskaia A (2004) Neotectonic evolution of the Anaximander Mountains at the junction of the Hellenic and Cyprus arcs, Tectonophysics 391: 35-65.

Woodside JM, Dumont JF, (1997) The Anaximander mountains are a southward rifted and foundered part of southwestern Turkish Taurus. Terra Nova 9: 394.

Woodside JM, Ivanov MK, Limonov AF and shipboard scientists of the Anaxiprobe expeditions (1998) Shallow gas and gas hydrates in the Anaximander Mountains region, eastern Mediterranean Sea. In: Gas Hydrates: Relevance to World Margin Stability and Climate Change (eds. Henriet JP and Mienert J) London, Geological Society. 137: 177-193.

Woodside JM, Mascle J, Zitter TAC, Limonov AF, Ergun M, and Volkonskaia A (2002) The Florence Rise, the western bend of the Cyprus Arc. Mar. Geol. 185: 177–194.

Zitter TAC, Huguen C, Woodside JM (2005) Geology of mud volcanoes in the eastern Mediterranean from combined sidescan sonar and submersible surveys. Deep-Sea Research I 52: 457-475.

Zitter TAC, Woodside JM and Mascle J (2003) The Anaximander Mountains: a clue to the tectonics of southwest Anatolia. Geological Journal, 38(3-4): 375-394.

10 Appendix: Station List

R/V POSEIDON P-462 — Station list

Station-number					Time (UTC)			Begin			End / off seafloor				
Ship-Station	GeoB	Instrument deployment-no.	Date 2013	Area	Begin	on ground	off off	End	Latitude N	Longitude E	Water (m)	Latitude N	Longitude E	Water (m)	Rec. (m)	Remarks Location, success,errors,.....
1024-1	17901-1	AUV-54a	02.11.	Thessaloniki MV	08:05			12:41	35° 28.71	30° 15.00	1249	35° 28.14	30° 15.87	1271		AUV dive was cancelled
1025-1	17902-1	SB-Profile	02.11.	Thessaloniki MV	13:57			14:30	35° 29.37	30° 13.75	1271	35° 29.38	30° 16.48	1353		First line of E-W survey over the MV
1026-1	17903-1	CTD-1	02.11.	Thessaloniki MV	14:41	15:11	15:11	15:38				35° 29.450	30° 16.850	1355		without water sampling, sl-max: 1343 m
1027-1	17904-1	SB-Profile	02.11.	Thessaloniki MV	15:47			20:56	35° 29.19	30° 16.73	1375	35° 27.87	30° 16.48			E-W survey over the MV
1028-1	17905-1	SB-Profile	03.11.	Anaximander	14:40			02:22	35° 44.73	30° 23.75		35° 28.88	30° 31.33			Filling gaps in the bathymetric map of the area
1029-1	17906-1	GC-1	04.11.	Thessaloniki MV	04:03	04:27	04:27	04:51				35° 28.723	30° 15.060	1240	5.00 m	On top of TMV, small GH pieces, 1 gas sample
1030-1	17907-1	GC-2	04.11.	Thessaloniki MV	06:00	06:24	06:24	06:48				35° 28.320	30° 15.960	1320	0.15 m	1 nm NE of TMV, carbonate layer and shells
1030-2	17907-2	GC-3	04.11.	Thessaloniki MV	07:05	07:25	07:25	07:47				35° 28.923	30° 15.964	1320	-	1 nm NE of TMV, only some sediment in core catcher
1031-1	17908-1	GC-4	04.11.	Thessaloniki MV	08:07	08:27	08:27	08:49				35° 28.553	30° 15.208	1258	3.40 m	On SE-Top of MV, GH sampled in 11 gas vials
1032-1	17909-1	GC-5	04.11.	Thessaloniki MV	09:27	09:46	09:46	10:10				35° 27.75	30° 15.19	1286	-	South of TMV, washed out
1033-1	17910-1	DAPC-1	04.11.	Thessaloniki MV	11:26	11:59	12:01	12:38				35° 28.538	30° 15.217	1243	-	SE-Top of TMV, same position as GC-4, failed
1034-1	17911-1	AUV-54b	04.11.	Thessaloniki MV	14:08			16:24	35° 28.52	30° 14.80	1278	35° 28.47	30° 14.70			AUV dive was cancelled
1035-1	17912-1	SB-Profile	04.11.	Anaximander	17:29			11:06	35° 24.23	30° 12.81		35° 26.72	30° 16.62			Passing AthMV, AMV, and KMV
1036-1	17913-1	DAPC-2	05.11.	Thessaloniki MV	11:53	12:36	12:36	13:15				35° 28.547	30° 15.204	1248		SE-top of TMV, same position as DAPC-1, failed
1037-1	17914-1	AUV-54c	05.11.	Thessaloniki MV	14:06			04:26	35° 28.51	30° 14.87		35° 28.92	30° 13.93			Dive successful, mission over TMV completed
1038-1	17915-1	SB-Profile	06.11.	Thessaloniki MV	05:12			07:24	35° 28.72	30° 13.20		35° 27.39	30° 13.22			Two E-W lines south of TMV to enlarge the mapped area
1039-1	17916-1	DAPC-3	06.11.	Thessaloniki MV	07:54	08:32	08:32	09:08				35° 28.555	30° 15.204	1241		SE-Top of TMV, same position as DAPC-1 and -2, failed
1040-1	17917-1	SB-Profile	06.11.	Thessaloniki MV	09:13			10:08	35° 28.57	30° 15.21	1248					Transit to Athina MV
1041-1	17918-1	GC-T-6	06.11.	Athina MV	10:39	11:11	11:20	11:48				35° 23.265	30° 12.610	1793	-	On AthMV, with 6 MTLs, carbonate crust in core catcher, no temp-data
1042-1	17919-1	SB-Profile	06.11.	Anaximander	12:11			15:54	35° 23.34	30° 12.49	1768	35° 24.18	30° 9.39			West of AthMV along the ridge crest
1043-1	17920-1	SB-Profile	06.11.	Anaximander	17:29			03:13				35° 32.99	30° 21.93			North of TMV, E-W lines
1044-1	17921-1	GC-T-7	07.11.	Thessaloniki MV	04:10	04:34	04:44	05:11				35° 27.984	30° 15.112	1296	1.20 m	S of TMV at mound, core bended, 6 MTLs - one lost, data from 4 MTLs
1045-1	17922-1	GC-8	07.11.	Thessaloniki MV	06:54	07:14	07:14	07:41				35° 28.270	30° 15.575	1303	1.50 m	BS-patch SE of Thessaloniki, no gas hydrates
1046-1	17923-1	GC-9	07.11.	Thessaloniki MV	08:03	08:22	08:22	08:46				35° 28.464	30° 15.581	1282	0.65 m	BS-patch east of TMV, carbonates and moussy sediment
1047-1	17924-1	GC-10	07.11.	Thessaloniki MV	10:01	10:21	10:21	10:54				35° 28.958	30° 15.391	1269	-	NE of TMV, carbonate in the core catcher, no sediment
1048-1	17925-1	GC-11	07.11.	Thessaloniki MV	11:29	11:47	11:47	12:13				35° 28.770	30° 14.960	1246	3.70 m	At NW peak at top of TMV, small pieces of gas hydrates, gas sampled in vials
1049-1	17926-1	GC-12	07.11.	Thessaloniki MV	12:41	13:04	13:04	13:25				35° 28.686	30° 15.067	1250		Flank northern summit at top of TMV, several layers already in the upper part of the core, gas sampled in vials
1050-1	17927-1	GC-13	07.11.	Thessaloniki MV	13:53	14:11	14:11	14:33				35° 28.558	30° 15.135	1239	1.90 m	At center of southern summit of Thessaloniki
1051-1	17928-1	SB-Profile	07.11.	Anaximander	16:18			5:15	35° 32.96	30° 21.96		35° 36.33	30° 20.78			Continuation of 1043-1, E-W lines north of TMV, bad weather
1052-1	17929-1	DAPC-4	08.11.	Thessaloniki MV	06:43	07:23	07:23	07:56				35° 28.685	30° 15.059	1245		failed
1053-1	17930-1	GC-14	08.11.	Kazan MV	09:53	10:23	10:23	10:49				35° 25.392	30° 33.673	1665	1.15 m	moussy sediments, no gas hydrates
1054-1	17931-1	GC-15	08.11.	Kazan MV	11:05	11:27	11:27	11:29				35° 25.879	30° 33.647	1665	1.64 m	Core full of dispersе gas hydrates but no larger pieces for sampling
1055-1	17932-1	GC-16	08.11.	Kazan MV	12:06	12:27	12:27	12:47				35° 25.88	30° 33.66	1664	2.30 m	Small pieces of gas hydrate
1056-1	17933-1	GC-17	08.11.	Kazan MV	13:10	13:29	13:29	13:48				35° 25.918	30° 33.660	1663	3.04 m	Small pieces of gas hydrate, gas sampled in vials
1057-1	17934-1	AUV-55	08.11.	Kazan MV	13:43			04:27	35° 26.27	30° 34.13		35° 25.94	30° 36.56			Mission ended after mapping the northern part of the planned dive
1058-1	17935-1	GC-18	09.11.	Athina MV	06:56	07:25	07:25	07:57				35° 23.603	30° 12.970	1761	0.95 m	Moussy but no hydrates, layer of carbonate precipitates. Top with bivalves
1059-1	17936-1	GC-19	09.11.	New MV	08:29	09:01	09:01	09:36				35° 22.313	30° 15.325	2005	-	Seep indicators in core catcher: carbonates, shells and a tubeworm
1060-1	17937-1	CTD-2	09.11.	South of AMV	10:30	11:06	11:06	11:37				35° 17.905	30° 16.564	2228		Down to 2100 m. T-sensor did not work properly
1061-1	17938-1	SB-Profile	09.11.	Anaximander	12:14			16:16				35° 26.06	30° 17.61			Mapping north of AMV and covering the newly mud volcano, just sampled
1062-1	17939-1	AUV-56	09.11.	Athina MV	17:51			20:40								Stopped mission shortly after first line on the seafloor
1063-1	17940-1	SB-Profile	09.11.	Anaximander	21:41			03:24	35° 25.97	30° 18.48		35° 25.00	30° 20.73			
1064-1	17941-1	GC-20	10.11.	Kazan MV	06:07	06:32	06:32	07:02				35° 26.011	30° 33.648	1669	1.18 m	Very dry, Full of small bright grey colored clasts
1065-1	17942-1	GC-21	10.11.	Kazan MV	07:33	08:01	08:01	08:28				35° 26.016	30° 33.669	1664	0.87 m	dry sedim., no gas hydrates, slightly moussy at the bottom, Light clasts
1066-1	17943-1	GC-22	10.11.	Kazan MV	08:45	09:09	09:09	09:38				35° 25.998	30° 33.667	1664	1.45 m	Between 100 and 145 cm full of dispersе gas hydrate but no larger pieces
1067-1	17944-1	AUV-57	10.11.	Athina MV	12:25			04:28	35° 23.55	30° 12.27		35° 24.70	30° 10.51			Dive successful
1068-1	17945-1	DAPC-5	11.11.	Kazan MV	06:53	07:41	7:41	08:10				35° 25.874	30° 33.653	1668	0.65 m	Pressure coring successful, recovery pressure ca. 190 bar, ca. 8500 ml gas

Appendix continued

Station-number					Time (UTC)				Begin			End / off seafloor				
Ship-Station	GeoB	Instrument deployment-no.	Date 2013	Area	Begin	on ground	off off	End	Latitude N	Longitude E	Water (m)	Latitude N	Longitude E	Water (m)	Rec. (m)	Remarks Location, success,errors,.....
1069-1	17946-1	GC-23	11.11.	Kazan MV	08:41	09:07	9:07	09:35				35°25.936	30°33.932	1711	0.45 m	mud breccia, no GH
1070-1	17947-1	GC-24	11.11.	Kazan MV	09:59	10:25	10:25	10:44				35°25.814	30°33.387	1704	2.28 m	core in line for archive
1071-1	17948-1	SB-Profile	11.11.	Anaximander	11:19			14:20				35° 23.81	30° 28.01			
1072-1	17949-1	AUV-58	11.11.	Amsterdam MV	16:48			07:54	35° 19.99	30° 16.15		35° 18.20	30° 16.19			Dive successful
1073-1	17950-1	GC-25	12.11.	Athina MV	08:55	09:24	09:24	09:54				35° 23.421	30° 13.204	1829	-	On eastern flank of the mud volcano, flare site, in core catcher fragments of carbonate crust and shells
1074-1	17951-1	GC-26	12.11.	Athina MV	10:31	10:58	10:58	11:29				35° 23.378	30° 13.285	1828	3.7 m	On eastern flank of the mud volcano, flare site, only few GH in core catcher
1075-1	17952-1	GC-27	12.11.	Athina MV	11:59	12:22	12:22	12:43				35° 23.568	30° 12.893	1777	3.6 m	At the proposed center of the mud volcano, core full of small gas hydrates
1075-2	17952-2	DAPC-6	12.11.	Athina MV	13:16	14:11	14:11	14:58				35° 23.575	30° 12.885	1777	?	Same position as GC-27, failed (maybe the resistivity of the sediment was insufficient for trigger weight)
1076-1	17953-1	SB-Profile	12.11.	Anaximander	16:31			02:58	35° 26.91	30° 22.54		35° 20.12	30° 19.50			Filling gaps in the bathymetric map between Amsterdam and Kazan MV
1077-1	17954-1	AUV-59	13.11.	Amsterdam MV	04:38			19:01	35° 19.89	30° 16.80		35° 19.32	30° 17.63			Successfully mapped the eastern part of the mud volcano
1078-1	17955-1	CTD-3	15.11.	Amsterdam MV	17:57	18:33	18:33	19:28				35°20.631	30°15.818	2005		To 1960 m depth, for calibrating T-sensors (did not work properly), and testing of a releaser failed
1079-1	17956-1	SB-Profile	15.11.	Anaximander	21:17			02:39	35° 20.66	30° 15.80	2033	35° 28.67	30° 31.58	1653		With less than 4 kn, but bridge forgot to shut off the 12 kHz deep sea echosounder (check quality due to disturbances)
1080-1	17957-1	CTD-4	16.11.	Athina MV	06:03	06:23	06:23	06:46				35°23.57	30°12.89	1774		Testing the releaser again, down to 1200 m, releaser worked
1080-2	17958-1	HF-1	16.11.	Athina MV	07:28	08:21	08:29					35°23.576	30°12.887	1830		First measurement at assumed centre or the MV: 80°C/km
1080-2	17958-2	HF-2	16.11.	Athina MV		08:51	08:59					35°23.549	30°12.859	1833		Second measurement: 50°C/km
1080-2	17958-3	HF-3	16.11.	Athina MV		09:26	09:34					35°23.495	30°12.820	1834		Third measurement: 30°C/km
1080-2	17958-4	HF-4	16.11.	Athina MV		10:08	10:17					35°23.379	30°12.779	1834		Fourth measurement: 50°C/km
1080-2	17958-5	HF-5	16.11.	Athina MV		10:43	10:53	11:20				35°23.312	30°12.913	1835		Fifth measurement: 26°C/km
1081-1	17959-1	AUV-60	16.11.	Amsterdam MV	13:40			04:31				35° 19.12	30° 15.75	2018		Successfully mapped the southern part of the mud volcano
1082-1	17960-1	CTD-5	17.11.	Athina MV	06:06	06:29	06:29	08:26				35° 23.58	30° 12.92	1774		Calibrating the T-sensors again, now it worked properly
1083-1	17961-1	SB-Profile	17.11.	Anaximander	08:51			12:59	35° 23.10	30° 11.45		35° 18.53	30° 7.01			Mapping the southwestern part of the working area
1084-1	17962-1	AUV-61	17.11.	Athina MV	15:00			04:40	35° 23.73	30° 12.75		35° 22.13	30° 15.22			Southern part of the AUV map achieved by AUV-57
1085-1	17963-1	HF-6	18.11.	Athina MV	06:01	06:39	06:48					35° 23.56	30° 12.87			
1085-1	17963-2	HF-7	18.11.	Athina MV		07:09	07:16					35° 23.61	30° 12.95			
1085-1	17963-3	HF-8	18.11.	Athina MV		07:59	08:00					35° 23.41	30° 13.21			Fallen on ground, no penetration
1085-1	17963-4	HF-9	18.11.	Athina MV		08:25	08:36	09:08				35° 23.37	30° 13.28			
1086-1	17964-1	GC-T-28	18.11.	Amsterdam MV	10:27	10:47	10:55	11:18				35° 19.246	30°15.194	2108	0.54 m	No GH
1087-1	17965-1	GC-T-29	18.11.	New MV	11:58	12:23	12:30	12:54				35° 22.433	30° 15.168		2.25 m	No GH
1088-1	17966-1	SB-Profile	18.11.	Anaximander	15:23			4,35	35° 24.99	30° 37.33		35° 35.23	30° 31.93			Mapping the western part of the working area
1089-1	17967-1	HF-10	19.11.	Kazan MV	06:06	06:51	06:59					35° 25.92	30° 33.94			
1089-1	17967-2	HF-11	19.11.	Kazan MV		07:30	07:39									
1089-1	17967-3	HF-12	19.11.	Kazan MV		07:55	08:02					35° 25.87	30° 33.65			
1089-1	17967-4	HF-13	19.11.	Kazan MV		08:16	08:24					35° 25.92	30° 33.66			
1089-1	17967-5	HF-14	19.11.	Kazan MV		08:35	08:42					35° 25.96	30° 33.66			
1089-1	17967-6	HF-15	19.11.	Kazan MV		09:00	09:07					35° 26.00	30° 33.65			First attempt fallen on ground
1089-1	17967-7	HF-16	19.11.	Kazan MV		09:20	09:27	09:48				35° 26.03	30° 33.66			

AUV	Autonomous Underwater Vehicle
GC	Gravity Corer
GC-T	Gravity Corer with MTLs
DAPC	Dynamic Autoclave Piston Corer
CTD	CTD hydrocast
SB	SEABEAM survey
SVP	Sound Velocity Profile
HF	Temperature lance with MTLs

From report No. 289 onwards this series is published under the new title:
Berichte aus dem MARUM und dem Fachbereich Geowissenschaften der Universität Bremen
A complete list of all publications of this series from no. 1 to 292 (1986 – 2012) was printed at last in issue no. 292.

No. 289 – Mohtadi, M. and cruise participants (2012). Report and preliminary results of RV SONNE Cruise SO 223T. TransGeoBiOc. Pusan – Suva, 09.09.2012 – 08.10.2012. 47 pages.

No. 290 – Hebbeln, D., Wienberg, C. and cruise participants (2012). Report and preliminary results of R/V Maria S. Merian cruise MSM20-4. WACOM – West-Atlantic Cold-water Corals Ecosystems: The West Side Story. Bridgetown – Freeport, 14 March – 7 April 2012. 120 pages.

No. 291 – Sahling, H. and cruise participants (2012). R/V Heincke Cruise Report HE-387. Gas emissions at the Svalbard continental margin. Longyearbyen – Bremerhaven, 20 August – 16 September 2012. 170 pages.

No. 292 – Pichler, T., Häusler, S. and Tsuonis, G. (2013). Abstracts of the 3rd International Workshop "Research in Shallow Marine and Fresh Water Systems". 134 pages.

No. 293 – Kucera, M. and cruise participants (2013). Cruise report of RV Sonne Cruise SO-226-3. Dip-FIP - The extent and structure of cryptic diversity in morphospecies of planktonic Foraminifera of the Indopacific Warm Pool. Wellington – Kaohsiung, 04.03.2013 - 28.03.2013. 39 pages.

No. 294 – Wienberg, C. and cruise participants (2013). Report and preliminary results of R/V Poseidon cruise P451-2. Practical training cruise onboard R/V Poseidon - From cruise organisation to marine geological sampling: Shipboard training for PhD students on R/V Poseidon in the Gulf of Cádiz, Spain. Portimao – Lisbon, 24 April – 1 May 2013. 65 pages.

No. 295 – Mohtadi, M. and cruise participants (2013). Report and preliminary results of R/V SONNE cruise SO-228, Kaohsiung-Townsville, 04.05.2013-23.06.2013, EISPAC-WESTWIND-SIODP. 107 pages.

No. 296 – Zonneveld, K. and cruise participants (2013). Report and preliminary results of R/V POSEIDON cruise POS448. CAPRICCIO – Calabrian and Adriatic Past River Input and Carbon ConversIOn In the Eastern Mediterranean. Messina – Messina, 6 – 23 March 2013. 47 pages.

No. 297 – Kopf, A. and cruise participants (2013). Report and preliminary results of R/V SONNE cruise SO222. MEMO: MeBo drilling and in situ Long-term Monitoring in the Nankai Trough accretionary complex, Japan. Leg A: Hong Kong, PR China, 09.06.2012 – Nagoya, Japan, 30.06.2012. Leg B: Nagoya, Japan, 04.07.2012 – Pusan, Korea, 18.07.2012. 121 pages.

No. 298 – Fischer, G. and cruise participants (2013). Report and preliminary results of R/V POSEIDON cruise POS445. Las Palmas – Las Palmas, 19.01.2013 – 01.02.2013. 30 pages.

No. 299 – Hanebuth, T.J.J. and cruise participants (2013). CORIBAR – Ice dynamics and meltwater deposits: coring in the Kveithola Trough, NW Barents Sea. Cruise MSM30. 16.07. – 15.08.2013, Tromsø (Norway) – Tromsø (Norway). 74 pages.

No. 300 – Bohrmann, G. and cruise participants (2014). Report and Preliminary Results of R/V POSEIDON Cruise P462, Izmir – Izmir, 28 October – 21 November, 2013. Gas Hydrate Dynamics of Mud Volcanoes in the Submarine Anaximander Mountains (Eastern Mediterranean). 51 pages.